humanized SCID mice profoundly reduced or abrogated parasitemia. These inhibitory effects were related to the antibody reactivity with the parasite native protein, which was seen in 60% of the volunteers, and remained in samples taken one year postimmunization.[3]

The blood-stage antigen SERA5 (for a review see ref. 4) is a promising blood-stage vaccine candidate against *P. falciparum*. SERA5 is largely produced during the late trophozoite and schizont stages.[5-7] Recombinant SE47' antigen, based on the SERA5 molecule, conferred protective immunity against parasite challenge in both *Aotus* and squirrel monkeys.[8-11] Mouse and rat antibodies against the SE47', likewise, inhibited parasite growth in vitro.[12-14] However, SE47' is highly hydrophobic, making large-scale manufacturing under good manufacturing practice (GMP) conditions a major challenge. Therefore, we constructed a new recombinant antigen, SE36, lacking the serine repeats. SE36 absorbed to the adjuvant aluminum hydroxide gel (SE36/AHG) was prepared under GMP conditions. SE36/AHG was highly immunogenic and anti-SE36 IgG titers lasted more than 1 y in chimpanzees.[15] Squirrel monkeys vaccinated with SE36/AHG were protected against high parasitemia, and serum anti-SE36 IgG titers were boosted after malaria parasite challenge. A human phase 1a clinical trial in Japan demonstrated that SE36/AHG (100 μg/1,000 μg) was safe, well-tolerated and immunogenic.[15] However, the mean titer of induced anti-SE36 antibody in the phase 1a trial was lower than that in African high responders.

Synthetic oligodeoxyribonucleotides (ODNs) containing immunostimulatory unmethylated cytosine-guanosine dinucleotides (CpG motifs) are potentially useful adjuvants and have been evaluated for veterinary and human vaccines.[16] These so-called CpG ODNs are categorized into two major classes, K- and D-type. K-type ODNs trigger the maturation of dendritic cells and stimulate the production of IgM and interleukin (IL)-6.[17,18] The D-type ODNs trigger antigen-presenting cell (APC) maturation and preferentially induce interferon (IFN)-α and -γ secretion.[18,19] It has been reported that K3 ODN effectively induces IL-6 production and cell proliferation, and that D35 ODN effectively secretes IFN-α in rhesus macaques.[20]

Another TLR9 ligand, synthetic hemozoin (sHZ, also known as β-hematin), is also a potent adjuvant for malarial antigens.[21] Hemozoin, a malaria pigment, is a detoxified product of heme molecules found in food vacuoles of the malaria parasites.[22,23] In previous studies, it was shown that purified HZ activates macrophages, thereby producing pro-inflammatory cytokines, chemokines and nitric oxide. HZ has also been shown to enhance human myeloid dendritic cell maturation.[21,24] Furthermore, the adjuvant function of sHZ was validated in a canine antiallergenic vaccine model.[25] Thus, HZ can influence adaptive immune responses to malaria infection and may have therapeutic value in vaccine adjuvant development.

We recently determined that a formulation of K3 and D35 ODNs, or sHZ with SE36/AHG was effective for the induction of anti-SE36 IgG in a rodent malaria model (Tougan et al., unpublished data). The purpose of this study was to increase the levels of induced antibody using a vaccine formulation containing TLR9 ligands as adjuvants. Here, we report the safety, immunogenicity and protective efficacy of the SE36/AHG formulation containing either K3 ODN, D35 ODN or sHZ as an adjuvant in non-human primate models.

Results

Adjuvant efficacy of TLR9 ligands to SE36/AHG. The adjuvant efficacy of K3 and D35 ODNs, and sHZ with SE36/AHG was examined. Twelve cynomolgus monkeys were randomly assigned to four groups. SE36/AHG, with or without each adjuvant, was administered four times and SE36-specific IgG titer was measured. Two weeks after the second immunization (Day 36), mean anti-SE36 antibody titers were 54.5, 432.9 ($p < 0.05$), 68.8 and 270.1 in the SE36/AHG, SE36/AHG with K3 ODN, SE36/AHG with D35 ODN and SE36/AHG with sHZ groups, respectively (**Fig. 1A and B**). Two weeks after the third immunization (Day 112), mean antibody titers were 182.2, 2258.9 ($p < 0.05$), 704.3 and 1276.1, respectively (**Fig. 1A and B**). Two weeks after the fourth immunization (Day 379), mean antibody titers were 237.8, 1960.8 ($p < 0.05$), 548.2 and 791.3 in the respective groups (**Fig. 1A and B**). At the three time points post-administration (**Fig. 1A and B**), the formulations including K3 ODN and sHZ elicited significantly higher anti-SE36 antibody titers. In particular, K3 ODN remarkably enhanced the antibody response after each administration. Furthermore, titers in individual monkeys from each group were compared immediately before each immunization to observe sustainability of the antibody titers. After the second immunization, mean antibody titers were 13.9, 176.0, 17.3 and 43.0 in the SE36/AHG, SE36/AHG with K3 ODN, SE36/AHG with D35 ODN, and SE36/AHG with sHZ groups, respectively (**Fig. 1A and B**). After the third immunization, mean antibody titers were 17.6, 157.7, 26.6 and 21.3, respectively (**Fig. 1A and B**). After the fourth immunization, mean antibody titers were 24.6, 164.5, 94.1 and 24.9 in the respective groups (**Fig. 1A and B**). These results indicate that the formulation with K3 ODN, but not sHZ, was able to sustain antibody titers although both were able to elicit statistically significant titers at each immunization time point.

Overall, the formulation of K3 ODN with SE36/AHG most effectively induced and maintained SE36-specific IgG titers. Additionally, there was no statistically significant difference between titers after the third or fourth immunization, with means of 1960.8 and 2258.9, respectively. This result suggests that an initial immunization with two boosters should be sufficient to confer the maximum levels of antibody titer (**Fig. 1A and B**).

Cytokine responses to SE36 stimulation. To examine the involvement of SE36-specific helper T cell responses, we measured cytokine secretion from peripheral blood mononuclear cells (PBMCs) 2 weeks after the second and fourth immunizations. IFN-γ was used as a marker of the Th1 response, IL-5 and IL-13 as markers of the Th2 response, and IL-17 as a marker of the Th17 response [Day 36 (i) and Day 379 (v) in **Fig. 1**]. On Day 36, IFN-γ was significantly induced in the SE36/AHG with K3 ODN group. IL-5 and IL-13 were significantly induced in each group where K3 ODN or sHZ was employed. These results suggest that a formulation containing K3 ODN promotes both Th1 and Th2 responses.

It appears that sHZ promotes the Th2 response only (**Fig. 2A**). On Day 379, IFN-γ, IL-5 and IL-13 were induced in groups containing K3 ODN in the formulation, along with the SE36/AHG and sHZ groups. These results indicate that four immunizations promote both Th1 and Th2 responses. IL-17 was induced in all four groups on Day 36, with cytokines significantly induced in SE36/AHG and sHZ groups, but only slightly induced in groups where K3 ODN and D35 ODN was included in the formulation (**Fig. 2B**). Of interest to us, the production of all cytokines was not prominent in the SE36/AHG with D35 ODN group at both time points despite the clear antibody titer induction in this group.

Immunostimulation using crude extracts of *P. falciparum*. To examine whether SE36-specific IgGs can be boosted by natural SERA5 antigen exposure after natural infection, we injected a crude extract of *P. falciparum* strain 3D7 into cynomolgus monkeys to mimic the complex mixture of *Plasmodium* antigens encountered during natural infection. The crude extract was administered at Day 583 (**Fig. 1**) and SE36-specific IgG titers were measured at 0 (Day 583), 1 and 2 weeks after injection. Although there was no statistical difference between week 1 and 2, in all groups, SE36-specific IgG titers were enhanced after injection (**Fig. 3**). We, thus, speculate that SE36-specific IgG antibodies could be boosted by malaria infection.

Vaccine trial in squirrel monkeys. To examine whether the formulation containing K3 ODN provided protective immunity against *P. falciparum* or not, a challenge experiment using squirrel monkeys was performed. At nine weeks after the first administration of the vaccine, blood-stage malaria challenge was done by intravenous injection of 5×10^8 infected red blood cells. It is worth mentioning that the formulation containing K3 ODN did not result in significantly higher antibody titers, which differed from the results we observed in cynomolgus monkeys (**Fig. 4A**).

All three monkeys immunized with SE36/AHG combined with K3 ODN, and one monkey immunized with SE36/AHG alone developed less than 30% parasitemia (maximum parasitemia: 22.6%, 26.8% and 13.3% in the SE36/AHG with K3 ODN group; and 22.0% in the SE36/AHG group). One monkey immunized with SE36/AHG, and two monkeys immunized with AHG combined with K3 ODN experienced fulminant infections of 40–50% parasitemia (maximum parasitemia: 42.3% in the SE36/AHG group and 47.6% and 47.8% in the

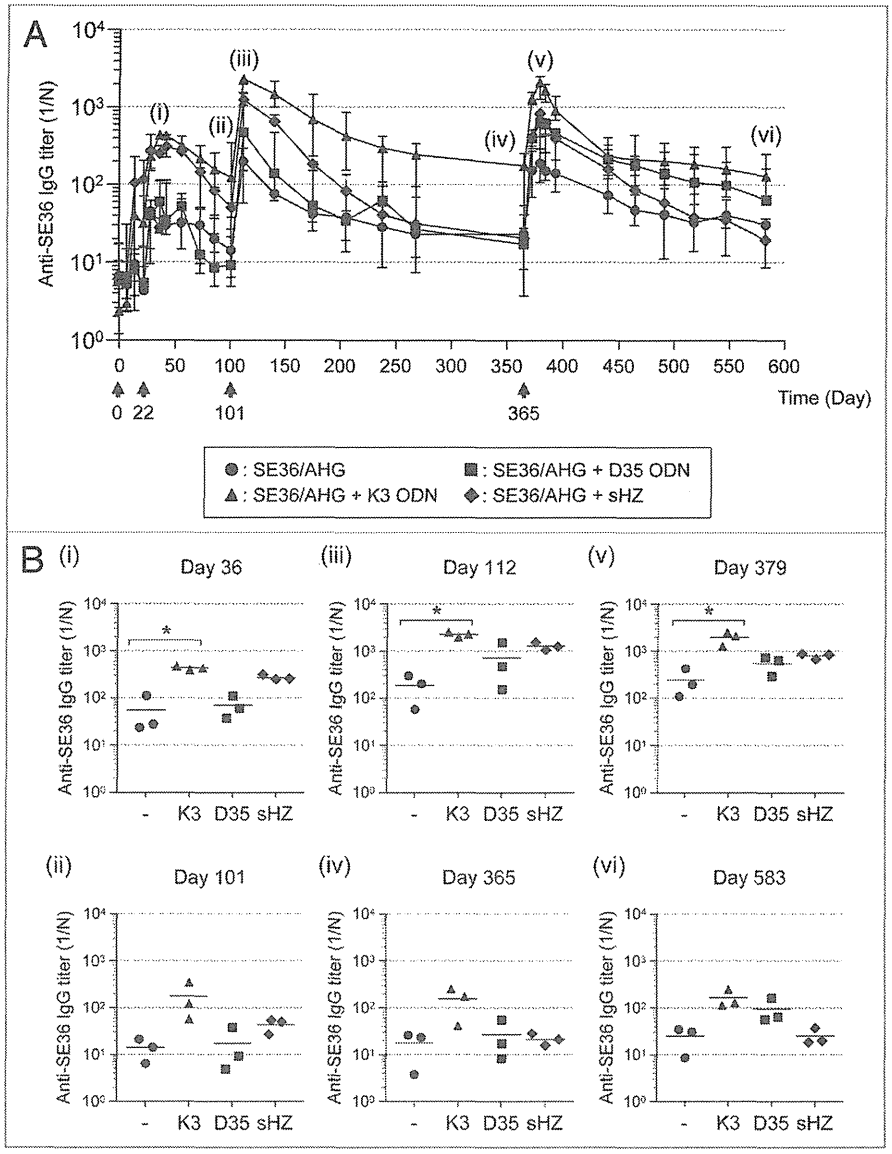

Figure 1. Formulation with K3 ODN effectively enhances SE36-specific IgG titers. (**A**) Time-course of SE36-specific IgG antibody titer. Cynomolgus monkeys were administered the same dose on days 0, 22, 101 and 365 (arrows). Sera were collected on days 0, 7, 14, 22, 28, 36, 42, 56, 73, 86, 101, 112, 140, 175, 205, 238, 268, 365, 372, 379, 384, 393, 440, 464, 491, 518, 547 and 583. Closed circles, triangles, squares and diamonds show the median titers (n = 3/group) of SE36/AHG, SE36/AHG with K3 ODN, SE36/AHG with D35 ODN and SE36/AHG with sHZ, respectively. Ranges are shown by bars. (**B**) Titers for individual monkeys subjected to different treatments on days 36 (i), 101 (ii), 112 (iii), 365 (iv), 379 (v) and 583 (vi) are compared. Statistical analysis for four groups was performed using non-parametric ANOVA (Kruskal-Wallis) with Dunn's post-hoc test; * indicates significant difference, $p < 0.05$.

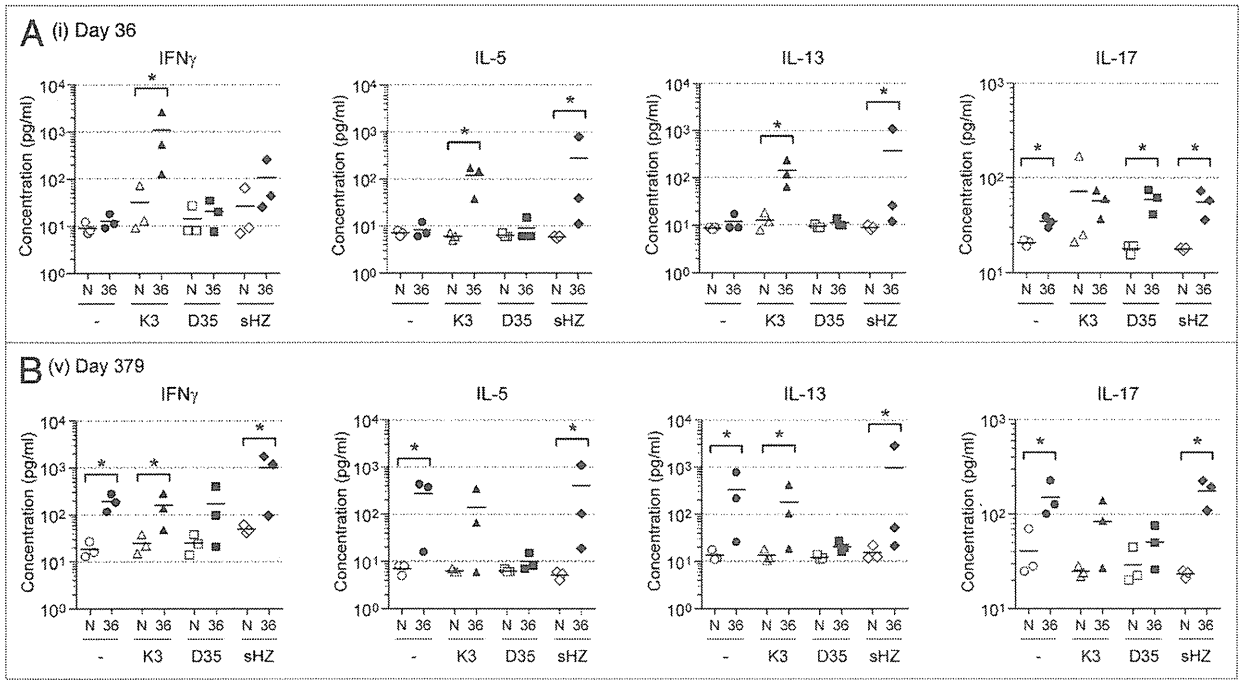

Figure 2. Cytokine response of PBMCs after stimulation with SE36 antigen in vitro. Levels in an individual cynomolgus monkey's cytokine (IFN-γ, IL-5, IL13 and IL-17) responses on days 36 (i) and 379 (v) are shown. "N" and "36" refer to non-stimulated (open symbols), and stimulated with SE36 (closed symbols), respectively. Closed circles, triangles, squares and diamonds indicate SE36/AHG, SE36/AHG with K3 ODN, SE36/AHG with D35 ODN and SE36/AHG with sHZ, respectively. Statistical analysis between pre- and post-immunization serum was performed using a Mann-Whitney U test. * indicates significant difference from the non-stimulated group, $p < 0.05$.

AHG with K3 ODN group) and were euthanized by Day 9 after challenge infection (**Fig. 4B**). These results indicate that the combined SE36/AHG with K3 ODN formulation afforded a level of protection that could substantially inhibit parasite growth. In the absence of robust statistical power, additional characterization of the induced anti-SE36 antibodies by the different treatments would be useful and could provide support for the observed correlation in the boosting of SE36-specific IgG titers after challenge infection and inhibition of parasite growth. Further in vitro assays would need to be incorporated in future studies.

To observe the importance of the anti-SE36 IgG antibody response, IgG titers against whole malaria parasite antigens were measured. For this purpose IgG titers against crude extract were measured after challenge infection. The IgG titers were immediately enhanced in all monkeys after challenge infection in contrast to responses of the anti-SE36 IgG titers (Tougan et al., unpublished data).

No serious adverse events during the studies were observed in both cynomolgus and squirrel monkeys. Common adverse reactions related to K3 ODN, such as erythema, swelling, induration or pruritus, were rarely detected at administration sites.

Discussion

Immunostimulatory CpG ODNs and sHZ that effect human immune cells in vitro often have limited immune-activating properties in mice. Relevant animal models such as non-human primates allow us the opportunity to demonstrate the safety and adjuvant activity of CpG ODNs and sHZ in vivo. In this study, we used cynomolgus and squirrel monkeys to evaluate the adjuvant efficacy of three TLR9 ligand adjuvants. In cynomolgus monkeys, all combined formulations of adjuvants with SE36/AHG enhanced SE36-specific IgG responses. In particular, the formulation with K3 ODN elicited over a 10-fold difference compared with SE36/AHG alone (**Fig. 1**). In **Figure 2**, it appears that formulations with K3 ODN enhanced the functions of helper T cells compared with those observed for SE36/AHG alone.

To date, many studies have demonstrated that various cytokines modulate an immune response during malaria infection. An increase in pro-inflammatory Th1 cytokines, such as IFN-γ and IL-12, during the acute phase of uncomplicated falciparum malaria has been inferred to play roles that contribute to an early and effective immune response, limiting progression toward a more severe course of malaria in humans.[26] Vaccine formulations containing CpG ODNs predominantly enhance Th1-associated cytokines, but Th2 responses involving IL-4 and IL-13 are often associated with AHG in mice.[16,27-30] However, the influence of CpG ODNs on cytokine responses in non-human primates has not been well characterized. In the current study, it was observed that the SE36/AHG formulation containing K3 ODN induced mixed Th1/Th2 responses in cynomolgus monkeys (**Fig. 2**).

The possibility of fluctuating T cell responses during this vaccination period is not clear as we did not perform cytokine assays on Days 112 (iii), 101 (ii), 365 (iv) or 583 (vi). Although this limitation would need to be addressed in future studies, this phenomenon has also been reported in several malaria vaccine candidates in mice, including AMA1-C1/AHG formulated with CPG 7909.[31] and SPf66-loaded PLGA microparticles.[32] A vaccination boost with recombinant SERA protein was also shown to markedly increase serum antibody titers in mice that were previously immunized with SERA plasmid DNA by gene gun vaccination.[33] In a murine malaria vaccine model, administration of *P. yoelii* $MSP1_{19}$/AHG formulated with CPG 7909, which is K-type CpG, induced a mixed Th1/Th2 response that resulted in enhanced vaccine efficacy, suggesting that the mixed Th1/Th2 response confers protective immunity against blood-stage infection.[34]

SE36-specific IgG titers were generally enhanced in all individual monkeys after injection of crude extract (Fig. 3). SE36 recombinant protein is derived from the N-terminal region of SERA5 based on the Honduras-1 strain corresponding to amino acids 17–382 where the serine repeats were removed (deletion of amino acids 193–225).[15] Although increased anti-SE36 IgG titers among all groups were not statistically different (Fig. 3), from squirrel monkey trials the formulation of K3 ODN appears effective for growth inhibition in various strains (Fig. 4).

In squirrel monkeys, the formulation with K3 ODN did not result in a higher antibody titer compared with the original SE36/AHG formulation, although protection that correlates with decreased parasite density in *P. falciparum* challenge was observed (Fig. 4A and B). The measurement of various cytokines in squirrel monkeys is not a sufficient measure of efficacy because they exhibit low levels of cross-reactivity with human cytokines.[35] Therefore, the interpretation of protective efficacy against malaria growth in terms of immunological responses is currently limited. Because the squirrel monkey is a valuable animal model for malaria vaccine development, the establishment of immunological analysis systems must provide more robust information for understanding the correlation between protective immunity and malaria infection.

No serious adverse events during the studies were observed in both cynomolgus and squirrel monkeys. Common adverse reactions related to K3 ODN were rarely detected at administration sites. Although empirical, the K3 ODN adjuvant formulation exhibited an adequate safety profile, justifying further studies to evaluate humoral and cellular responses in humans. A number of clinical trials looking at CpG ODN formulations have been initiated in the field of malaria vaccine development. Formulations of K-type ODN, CpG 7909, with MSP1 and AMA1 effectively boost antigen-specific IgG levels and demonstrate an adequate safety profile.[36-39] In clinical trials for hepatitis B (Engerix-B) and flu (Fluarix) vaccines, enhanced safety and immunogenicity of CpG 7909 formulations have been reported.[40,41]

In conclusion, our study demonstrates that the formulation of K3 ODN with SE36/AHG can result in the improvement of immune response.

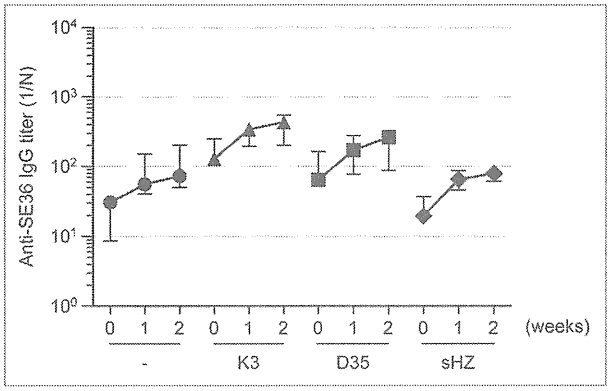

Figure 3. Trends in SE36-specific IgG antibody titers from cynomolgus monkeys after the mimic challenge infection. Crude extract was administered on day 583, and sera from each monkey were collected on day 583 (week 0), weeks 1 and 2. Median titers are represented by closed circles (SE36/AHG), triangles (SE36/AHG with K3 ODN), squares (SE36/AHG with D35 ODN) and diamonds (SE36/AHG with sHZ). Ranges are shown by bars. Statistical analysis at each timepoints (week 1 and 2) was performed using non-parametric ANOVA (Kruskal-Wallis) with Dunn's post-hoc test.

Materials and Methods

Animals, immunization and infection. A total of 12 cynomolgus monkeys (*Macaca fascicularis*) were obtained from Tsukuba Primate Research Center (TPRC), National Institute of Biomedical Innovation (NIBIO) and randomly assigned to four groups (n = 3/group). Animals were immunized subcutaneously on days 0, 22, 101 and 365 of our study with a mixture of 10 μg of SE36 and 125 μg of AHG with and without 500 μg of K3 ODN or D35 ODN in a total volume of 1 ml, or with 1.5 mM sHZ in a total volume of 1 ml. The SE36 antigen and AHG adjuvant were GMP-quality[15] and K3 and D35 ODNs and sHZ adjuvants were prepared specifically for this study. K3 and D35 were prepared as GMP quality by Gene Design Inc. and sHZ was prepared under sterile conditions with non-detectable endotoxin levels determined by LAL assay.

A total of seven squirrel monkeys (*Saimiri sciureus*) were purchased from PETSUN Co., Ltd. and randomly assigned to three groups: SE36/AHG (n = 2); SE36/AHG with K3 ODN (n = 3); and AHG with K3 ODN group (n = 2). These animals were subcutaneously immunized twice at a 3-week interval with a combination of 10 μg of SE36, 125 μg of AHG with or without 500 μg of K3 ODN in a total volume of 0.5 ml. The monkeys were splenectomized before inoculation. Nine weeks after the first immunization, parasite challenge experiments were done using the live IPC/Ray strain[42] (5×10^8 infected red blood cells) introduced intravenously in the saphenous vein. Parasitemia was monitored daily by counting 5,000 RBCs in Giemsa-stained thin blood smears. Drug treatment was commenced at Day 14, and in cases where parasitemia surpassed the set threshold parasitemia (40%) during the experimental period, the animal was euthanized to avoid sequelae, such as severe malaria, in accordance with the guidelines for animal welfare and care (Guidelines

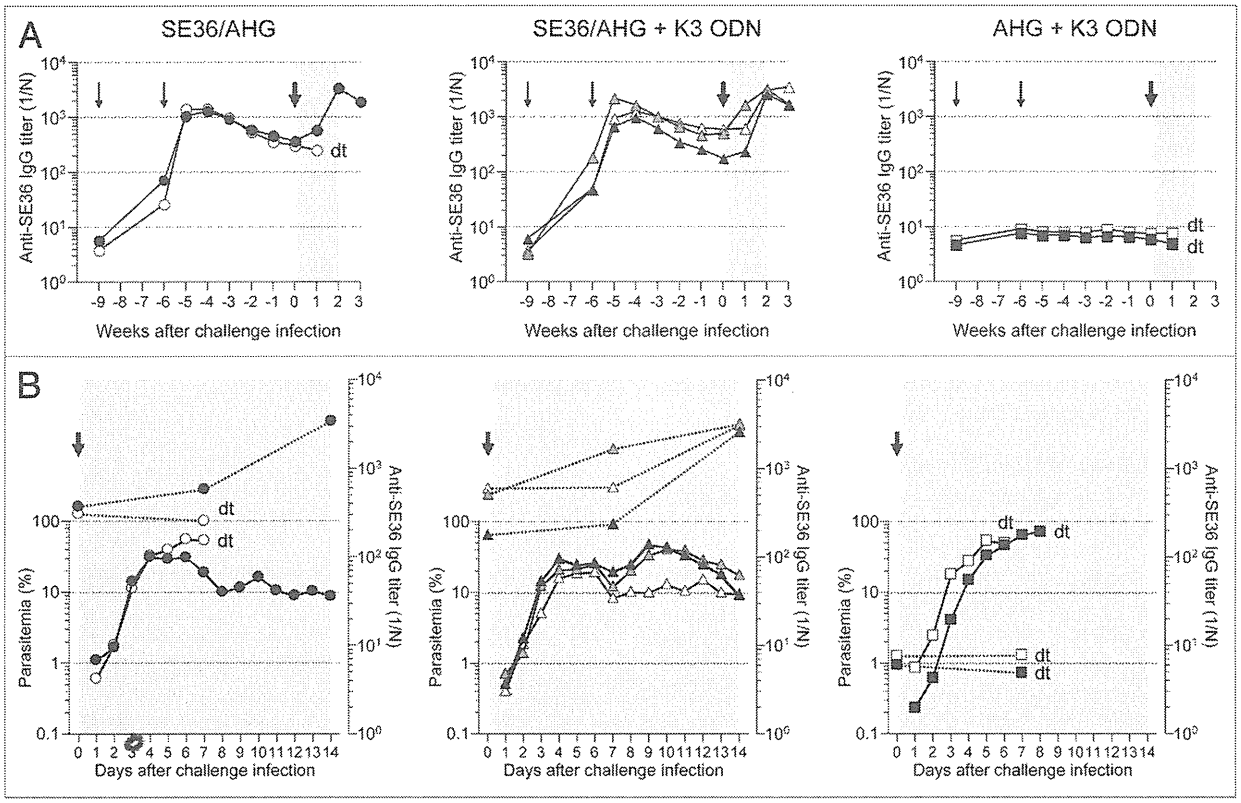

Figure 4. Vaccine trial in squirrel monkeys. **(A)** Time-course analysis of SE36-specific IgG antibody titer. Animals were administered 10 μg of SE36, 100 μg of AHG and/or 500 μg of K3 ODN at 6 and 9 weeks (thin arrows) before the challenge infection (bold arrow). **(B)** Time-course analysis of parasitemia. Parasite densities were measured up to 14 d after infection. Left Y-axis shows parasitemia and right Y-axis shows SE36-specific IgG antibody titers. Bold arrow shows the challenge infection. Dotted lines show the SE36-specific IgG antibody titers as in **(A)**. In **(A)** and **(B)**, light gray area shows duration of parasitemia measurement. The term "dt" denotes a monkey that was euthanized, or died owing to acute conditions. Groups are represented by closed circles (SE36/AHG), triangles (SE36/AHG with K3 ODN) and squares (AHG with K3 ODN). Black, gray and white symbols indicate the individual animals in each group.

for the Animal Care and Management of TPRC, NIBIO). All experimental protocols were approved by the Animal Welfare and Animal Care Committee at TPRC, NIBIO where animals were housed and handled. The vaccination schedule was identical to GLP studies and clinical trials for SE36 malaria vaccine.[15]

All experimental protocols were approved by the Animal Welfare and Animal Care Committee at TPRC, NIBIO. All animals were housed and handled in accordance with the Guidelines for Laboratory Animals at TPRC, NIBIO.

Adjuvants. The following human-type CpG ODNs were used: K3 ODN (ATCGACTCTCGAGCGTTCTC) and D35 ODN (GGtgcatcgatgcaggggGG). Bases shown in uppercase are phosphorothioate, and those in lowercase are phosphodiester, with CpG dinucleotides underlined.[20] These ODNs were purchased from GeneDesign Inc. The sHZ was purified from hemin chloride using the acid-catalyzed method to produce smaller and homogenous crystals as previously described.[24,25,43,44]

Antibody detection by indirect enzyme-linked immunosorbent assay (ELISA). An optimized concentration (1 μg/ml) of the recombinant SE36 antigen in carbonate/bi-carbonate buffer (pH 9.6) was used to coat wells of a 96-well MaxiSorp NUNC-Immuno plate (Nunc, Catalog number: 442404) overnight at 4°C. Plates were washed and blocked with 5% skim milk in phosphate-buffered saline (PBS) containing 0.05% Tween 20 for 2 h at room temperature. Cynomolgus monkey IgG was detected using horseradish peroxidase (HRP)-conjugated anti-monkey IgG (whole molecule) antibody produced in rabbit (Sigma-Aldrich, Catalog number: A2054). Squirrel monkey IgG was detected using anti-squirrel monkey IgG polyclonal antibody produced in rat (a kind gift from Dr. T. Tachibana) and HRP-conjugated anti-rat IgG (whole molecule) antibody produced in rabbit (Sigma-Aldrich, Catalog number: A5795). Color was developed using a TMB microwell peroxidase substrate (KPL, Catalog number: 50–76–00). The reaction was stopped with 1 M H_2SO_4. Absorbance was measured at 450/540 nm within 30 min using a SpectraMax 340PC[384] Microplate Reader (Molecular Devices).

Detection of Cytokines. PBMCs of cynomolgus monkeys were purified by Ficoll-Hypaque (GE Healthcare, Catalog number: 17–1440–02) gradient centrifugation from blood samples obtained at days 36 and 378. Isolated cells were stimulated with GMP-quality SE36 antigen or PBS at 37°C for 24 h. Cytokine

concentrations in the culture supernatant were determined using a Milliplex Non-Human Primate Cytokine Panel - Premixed 23 Plex (Millipore, Catalog number: MPXPRCYTO40KPX23).

Immunostimulation using crude extracts of *P. falciparum*. All cynomolgus monkeys were subcutaneously injected on Day 583 with 100 μl of crude 3D7 parasite lysate (21.5 mg/ml). Blood samples were drawn at 0 (Day 583), 1 and 2 weeks later and the amount of SE36-specific IgG antibodies measured by ELISA.

Statistical analysis. Comparisons of IgG titer data among groups of monkeys were performed by non-parametric ANOVA (Kruskal-Wallis) with Dunn's post-hoc test. Comparisons of cytokine levels between two groups were performed by non-parametric Mann-Whitney U test. Statistical analyses were performed using the Graphpad Prism 5 software package.

Disclosure of Potential Conflicts of Interest

T.T., K.J.I. and T.H. hold patent for production of BK-SE36/CpG.

Acknowledgments

We thank Dr. Taro Tachibana at Department of Bioengineering, Graduate School of Engineering, Osaka City University for anti-squirrel monkey IgG antibody. This work was supported by the New Energy and Industrial Technology Development Organization (NEDO) of Japan (97S08–011 to T.H.). This work was also supported by a grant from the Cooperative Link of Unique Science and Technology for Economy Revitalization (CLUSTER) promoted by the Ministry of Education, Culture, Sports and Technology (to T.H. and K.J.I.). And this work was partially supported by Grant-in-Aid for Young Scientists (B) (22700455) from the Japanese Ministry of Education, Science, Sports, Culture and Technology (to T.T.).

References

1. Coler RN, Carter D, Friede M, Reed SG. Adjuvants for malaria vaccines. Parasite Immunol 2009; 31:520-8; PMID:19691556; http://dx.doi.org/10.1111/j.1365-3024.2009.01142.x.
2. Stoute JA, Slaoui M, Heppner DG, Momin P, Kester KE, Desmons P, et al. A preliminary evaluation of a recombinant circumsporozoite protein vaccine against Plasmodium falciparum malaria. RTS,S Malaria Vaccine Evaluation Group. N Engl J Med 1997; 336:86-91; PMID:8988885; http://dx.doi.org/10.1056/NEJM199701093360202.
3. Druilhe P, Spertini F, Soesoe D, Corradin G, Mejia P, Singh S, et al. A malaria vaccine that elicits in humans antibodies able to kill Plasmodium falciparum. PLoS Med 2005; 2:e344; PMID:16262450; http://dx.doi.org/10.1371/journal.pmed.0020344.
4. Palacpac NM, Arisue N, Tougan T, Ishii KJ, Horii T. Plasmodium falciparum serine repeat antigen 5 (SE36) as a malaria vaccine candidate.Vaccine 2011; 29:5837-45; PMID:21718740; http://dx.doi.org/10.1016/j.vaccine.2011.06.052.
5. Bzik DJ, Li WB, Horii T, Inselburg J. Amino acid sequence of the serine-repeat antigen (SERA) of Plasmodium falciparum determined from cloned cDNA. Mol Biochem Parasitol 1988; 30:279-88; PMID:2847041; http://dx.doi.org/10.1016/0166-6851(88)90097-7.
6. Delplace P, Fortier B, Tronchin G, Dubremetz JF, Vernes A. Localization, biosynthesis, processing and isolation of a major 126 kDa antigen of the parasitophorous vacuole of Plasmodium falciparum. Mol Biochem Parasitol 1987; 23:193-201; PMID:3299083; http://dx.doi.org/10.1016/0166-6851(87)90026-0.
7. Fox BA, Bzik DJ. Analysis of stage-specific transcripts of the Plasmodium falciparum serine repeat antigen (SERA) gene and transcription from the SERA locus. Mol Biochem Parasitol 1994; 68:133-44; PMID:7891737; http://dx.doi.org/10.1016/0166-6851(94)00162-6.
8. Inselburg J, Bathurst IC, Kansopon J, Barchfeld GL, Barr PJ, Rossan RN. Protective immunity induced in Aotus monkeys by a recombinant SERA protein of Plasmodium falciparum: adjuvant effects on induction of protective immunity. Infect Immun 1993; 61:2041-7; PMID:8478092.
9. Inselburg J, Bathurst IC, Kansopon J, Barr PJ, Rossan R. Protective immunity induced in Aotus monkeys by a recombinant SERA protein of Plasmodium falciparum: further studies using SERA 1 and MF75.2 adjuvant. Infect Immun 1993; 61:2048-52; PMID:8478093.
10. Inselburg J, Bzik DJ, Li WB, Green KM, Kansopon J, Hahm BK, et al. Protective immunity induced in Aotus monkeys by recombinant SERA proteins of Plasmodium falciparum. Infect Immun 1991; 59:1247-50; PMID:1900809.
11. Suzue K, Ito M, Matsumoto Y, Tanioka Y, Horii T. Protective immunity induced in squirrel monkeys with recombinant serine repeat antigen (SERA) of Plasmodium falciparum. Parasitol Int 1997; 46:17-25; http://dx.doi.org/10.1016/S1383-5769(97)00004-4.
12. Pang XL, Mitamura T, Horii T. Antibodies reactive with the N-terminal domain of Plasmodium falciparum serine repeat antigen inhibit cell proliferation by agglutinating merozoites and schizonts. Infect Immun 1999; 67:1821-7; PMID:10085023.
13. Sugiyama T, Suzue K, Okamoto M, Inselburg J, Tai K, Horii T. Production of recombinant SERA proteins of Plasmodium falciparum in Escherichia coli by using synthetic genes. Vaccine 1996; 14:1069-76; PMID:8879104; http://dx.doi.org/10.1016/0264-410X(95)00238-V.
14. Fox BA, Xing-Li P, Suzue K, Horii T, Bzik DJ. Plasmodium falciparum: an epitope within a highly conserved region of the 47-kDa amino-terminal domain of the serine repeat antigen is a target of parasite-inhibitory antibodies. Exp Parasitol 1997; 85:121-34; PMID:9030663; http://dx.doi.org/10.1006/expr.1996.4118.
15. Horii T, Shirai H, Jie L, Ishii KJ, Palacpac NQ, Tougan T, et al. Evidences of protection against blood-stage infection of Plasmodium falciparum by the novel protein vaccine SE36. Parasitol Int 2010; 59:380-6; PMID:20493274; http://dx.doi.org/10.1016/j.parint.2010.05.002.
16. Klinman DM, Klaschik S, Sato T, Tross D. CpG oligonucleotides as adjuvants for vaccines targeting infectious diseases. Adv Drug Deliv Rev 2009; 61:248-55; PMID:19272313; http://dx.doi.org/10.1016/j.addr.2008.12.012.
17. Kadowaki N, Antonenko S, Liu YJ. Distinct CpG DNA and polyinosinic-polycytidylic acid double-stranded RNA, respectively, stimulate CD11c- type 2 dendritic cell precursors and CD11c+ dendritic cells to produce type I IFN. J Immunol 2001; 166:2291-5; PMID:11160284.
18. Verthelyi D, Ishii KJ, Gursel M, Takeshita F, Klinman DM. Human peripheral blood cells differentially recognize and respond to two distinct CPG motifs. J Immunol 2001; 166:2372-7; PMID:11160295.
19. Krug A, Rothenfusser S, Hornung V, Jahrsdörfer B, Blackwell S, Ballas ZK, et al. Identification of CpG oligonucleotide sequences with high induction of IFN-alpha/beta in plasmacytoid dendritic cells. Eur J Immunol 2001; 31:2154-63; PMID:11449369; http://dx.doi.org/10.1002/1521-4141(200107)31:7<2154::AID-IMMU2154>3.0.CO;2-U.
20. Verthelyi D, Kenney RT, Seder RA, Gam AA, Friedag B, Klinman DM. CpG oligodeoxynucleotides as vaccine adjuvants in primates. J Immunol 2002; 168:1659-63; PMID:11823494.
21. Coban C, Ishii KJ, Sullivan DJ, Kumar N. Purified malaria pigment (hemozoin) enhances dendritic cell maturation and modulates the isotype of antibodies induced by a DNA vaccine. Infect Immun 2002; 70:3939-43; PMID:12065539; http://dx.doi.org/10.1128/IAI.70.7.3939-3943.2002.
22. Arese P, Schwarzer E. Malarial pigment (haemozoin): a very active 'inert' substance. Ann Trop Med Parasitol 1997; 91:501-16; PMID:9329987; http://dx.doi.org/10.1080/00034989760879.
23. Sullivan DJ. Theories on malarial pigment formation and quinoline action. Int J Parasitol 2002; 32:1645-53; PMID:12435449; http://dx.doi.org/10.1016/S0020-7519(02)00193-5.
24. Coban C, Ishii KJ, Kawai T, Hemmi H, Sato S, Uematsu S, et al. Toll-like receptor 9 mediates innate immune activation by the malaria pigment hemozoin. J Exp Med 2005; 201:19-25; PMID:15630134; http://dx.doi.org/10.1084/jem.20041836.
25. Coban C, Igari Y, Yagi M, Reimer T, Koyama S, Aoshi T, et al. Immunogenicity of whole-parasite vaccines against Plasmodium falciparum involves malarial hemozoin and host TLR9. Cell Host Microbe 2010; 7:50-61; PMID:20114028; http://dx.doi.org/10.1016/j.chom.2009.12.003.
26. Torre D, Speranza F, Giola M, Matteelli A, Tambini R, Biondi G. Role of Th1 and Th2 cytokines in immune response to uncomplicated Plasmodium falciparum malaria. Clin Diagn Lab Immunol 2002; 9:348-51; PMID:11874876.
27. Chu RS, Targoni OS, Krieg AM, Lehmann PV, Harding CV. CpG oligodeoxynucleotides act as adjuvants that switch on T helper 1 (Th1) immunity. J Exp Med 1997; 186:1623-31; PMID:9362523; http://dx.doi.org/10.1084/jem.186.10.1623.
28. Jegerlehner A, Maurer P, Bessa J, Hinton HJ, Kopf M, Bachmann MF. TLR9 signaling in B cells determines class switch recombination to IgG2a. J Immunol 2007; 178:2415-20; PMID:17277148.

29. Klinman DM, Yi AK, Beaucage SL, Conover J, Krieg AM. CpG motifs present in bacteria DNA rapidly induce lymphocytes to secrete interleukin 6, interleukin 12, and interferon gamma. Proc Natl Acad Sci U S A 1996; 93:2879-83; PMID:8610135; http://dx.doi.org/10.1073/pnas.93.7.2879.
30. Lin L, Gerth AJ, Peng SL. CpG DNA redirects class-switching towards "Th1-like" Ig isotype production via TLR9 and MyD88. Eur J Immunol 2004; 34:1483-7; PMID:15114682; http://dx.doi.org/10.1002/eji.200324736.
31. Mullen GE, Giersing BK, Ajose-Popoola O, Davis HL, Kothe C, Zhou H, et al. Enhancement of functional antibody responses to AMA1-C1/Alhydrogel, a Plasmodium falciparum malaria vaccine, with CpG oligodeoxynucleotide. Vaccine 2006; 24:2497-505; PMID:16434128; http://dx.doi.org/10.1016/j.vaccine.2005.12.034.
32. Carcaboso AM, Hernández RM, Igartua M, Rosas JE, Patarroyo ME, Pedraz JL. Potent, long lasting systemic antibody levels and mixed Th1/Th2 immune response after nasal immunization with malaria antigen loaded PLGA microparticles. Vaccine 2004; 22:1423-32; PMID:15063565; http://dx.doi.org/10.1016/j.vaccine.2003.10.020.
33. Belperron AA, Feltquate D, Fox BA, Horii T, Bzik DJ. Immune responses induced by gene gun or intramuscular injection of DNA vaccines that express immunogenic regions of the serine repeat antigen from Plasmodium falciparum. Infect Immun 1999; 67:5163-9; PMID:10496891.
34. Near KA, Stowers AW, Jankovic D, Kaslow DC. Improved immunogenicity and efficacy of the recombinant 19-kilodalton merozoite surface protein 1 by the addition of oligodeoxynucleotide and aluminum hydroxide gel in a murine malaria vaccine model. Infect Immun 2002; 70:692-701; PMID:11796601; http://dx.doi.org/10.1128/IAI.70.2.692-701.2002.
35. Ozwara H, Niphuis H, Buijs L, Jonker M, Heeney JL, Bambra CS, et al. Flow cytometric analysis on reactivity of human T lymphocyte-specific and cytokine-receptor-specific antibodies with peripheral blood mononuclear cells of chimpanzee (Pan troglodytes), rhesus macaque (Macaca mulatta), and squirrel monkey (Saimiri sciureus). J Med Primatol 1997; 26:164-71; PMID:9379483; http://dx.doi.org/10.1111/j.1600-0684.1997.tb00048.x.
36. Ellis RD, Martin LB, Shaffer D, Long CA, Miura K, Fay MP, et al. Phase 1 trial of the Plasmodium falciparum blood stage vaccine MSP1(42)-C1/Alhydrogel with and without CPG 7909 in malaria naïve adults. PLoS One 2010; 5:e8787; PMID:20107498; http://dx.doi.org/10.1371/journal.pone.0008787.
37. Ellis RD, Mullen GE, Pierce M, Martin LB, Miura K, Fay MP, et al. A Phase 1 study of the blood-stage malaria vaccine candidate AMA1-C1/Alhydrogel with CPG 7909, using two different formulations and dosing intervals. Vaccine 2009; 27:4104-9; PMID:19410624; http://dx.doi.org/10.1016/j.vaccine.2009.04.077.
38. Mullen GE, Ellis RD, Miura K, Malkin E, Nolan C, Hay M, et al. Phase 1 trial of AMA1-C1/Alhydrogel plus CPG 7909: an asexual blood-stage vaccine for Plasmodium falciparum malaria. PLoS One 2008; 3:e2940; PMID:18698359; http://dx.doi.org/10.1371/journal.pone.0002940.
39. Sagara I, Ellis RD, Dicko A, Niambele MB, Kamate B, Guindo O, et al. A randomized and controlled Phase 1 study of the safety and immunogenicity of the AMA1-C1/Alhydrogel + CPG 7909 vaccine for Plasmodium falciparum malaria in semi-immune Malian adults. Vaccine 2009; 27:7292-8; PMID:19874925; http://dx.doi.org/10.1016/j.vaccine.2009.10.087.
40. Cooper CL, Davis HL, Morris ML, Efler SM, Adhami MA, Krieg AM, et al. CPG 7909, an immunostimulatory TLR9 agonist oligodeoxynucleotide, as adjuvant to Engerix-B HBV vaccine in healthy adults: a double-blind phase I/II study. J Clin Immunol 2004; 24:693-701; PMID:15622454; http://dx.doi.org/10.1007/s10875-004-6244-3.
41. Cooper CL, Davis HL, Morris ML, Efler SM, Krieg AM, Li Y, et al. Safety and immunogenicity of CPG 7909 injection as an adjuvant to Fluarix influenza vaccine. Vaccine 2004; 22:3136-43; PMID:15297066; http://dx.doi.org/10.1016/j.vaccine.2004.01.058.
42. Groux H, Perraut R, Garraud O, Poingt JP, Gysin J. Functional characterization of the antibody-mediated protection against blood stages of Plasmodium falciparum in the monkey Saimiri sciureus. Eur J Immunol 1990; 20:2317-23; PMID:2242760; http://dx.doi.org/10.1002/eji.1830201022.
43. Egan TJ. Recent advances in understanding the mechanism of hemozoin (malaria pigment) formation. J Inorg Biochem 2008; 102:1288-99; PMID:18226838; http://dx.doi.org/10.1016/j.jinorgbio.2007.12.004.
44. Jaramillo M, Godbout M, Olivier M. Hemozoin induces macrophage chemokine expression through oxidative stress-dependent and -independent mechanisms. J Immunol 2005; 174:475-84; PMID:15611273.

BASIC AND TRANSLATIONAL—LIVER

A Serine Palmitoyltransferase Inhibitor Blocks Hepatitis C Virus Replication in Human Hepatocytes

ASAO KATSUME,[1,2,*] YUKO TOKUNAGA,[1,*] YUICHI HIRATA,[1] TSUBASA MUNAKATA,[1] MAKOTO SAITO,[1] HITOHISA HAYASHI,[1] KOICHI OKAMOTO,[2] YUSUKE OHMORI,[2] ISAMU KUSANAGI,[3] SHINYA FUJIWARA,[2] TAKUO TSUKUDA,[2] YUKO AOKI,[2] KLAUS KLUMPP,[4] KYOKO TSUKIYAMA-KOHARA,[5] AHMED EL-GOHARY,[6] MASAYUKI SUDOH,[2] and MICHINORI KOHARA[1]

[1]Department of Microbiology and Cell Biology, Tokyo Metropolitan Institute of Medical Science, Tokyo, Japan; [2]Research Division, Chugai Pharmaceutical Co., Ltd., Tokyo, Japan; [3]Chugai Research Institute for Medical Science Inc., Kanagawa, Japan; [4]F. Hoffmann-La Roche Inc., Nutley, New Jersey; [5]Transboundary Animal Diseases Center, Joint Faculty of Veterinary Medicine, Kagoshima University, Kagoshima, Japan; and [6]Department of Clinical Pathology, Faculty of Medicine Suez Canal University, Ismailia, Egypt

See Covering the Cover synopsis on page 701.

BACKGROUND & AIMS: Host cell lipid rafts form a scaffold required for replication of hepatitis C virus (HCV). Serine palmitoyltransferases (SPTs) produce sphingolipids, which are essential components of the lipid rafts that associate with HCV nonstructural proteins. Prevention of the de novo synthesis of sphingolipids by an SPT inhibitor disrupts the HCV replication complex and thereby inhibits HCV replication. We investigated the ability of the SPT inhibitor NA808 to prevent HCV replication in cells and mice. **METHODS:** We tested the ability of NA808 to inhibit SPT's enzymatic activity in FLR3-1 replicon cells. We used a replicon system to select for HCV variants that became resistant to NA808 at concentrations 4- to 6-fold the 50% inhibitory concentration, after 14 rounds of cell passage. We assessed the ability of NA808 or telaprevir to inhibit replication of HCV genotypes 1a, 1b, 2a, 3a, and 4a in mice with humanized livers (transplanted with human hepatocytes). NA808 was injected intravenously, with or without pegylated interferon alfa-2a and HCV polymerase and/or protease inhibitors. **RESULTS:** NA808 prevented HCV replication via noncompetitive inhibition of SPT; no resistance mutations developed. NA808 prevented replication of all HCV genotypes tested in mice with humanized livers. Intravenous NA808 significantly reduced viral load in the mice and had synergistic effects with pegylated interferon alfa-2a and HCV polymerase and protease inhibitors. **CONCLUSIONS: The SPT inhibitor NA808 prevents replication of HCV genotypes 1a, 1b, 2a, 3a, and 4a in cultured hepatocytes and in mice with humanized livers. It might be developed for treatment of HCV infection or used in combination with pegylated interferon alfa-2a or HCV polymerase or protease inhibitors.**

Keywords: Direct-Acting Antiviral Agents; DAAs; HCV Lifecycle; Drug.

Hepatitis C virus (HCV) is a major cause of morbidity, affecting approximately 170 million people worldwide.[1] In many cases, HCV results in a persistent infection that evades the host immune response, leading to chronic liver disease, chronic hepatitis, cirrhosis, and hepatocellular carcinoma.[2]

The current therapy for chronic hepatitis C is a combination of weekly injections of pegylated interferon alfa-2a (PEG-IFN) and twice-daily oral doses of ribavirin (RBV). Unfortunately, this combination therapy has limited efficacy and significant side effects.[3,4] Although the HCV NS3/4A protease inhibitors telaprevir and SCH503034 (boceprevir) are approved for the treatment of chronic HCV infection, these compounds must be combined with the current standard of care to be efficacious, and they cannot cure all infected individuals, including IFN-intolerant patients.[5–7] Therefore, antiviral combinations that can achieve superior sustained virologic response without the use of IFN or RBV are needed.

IFN-free combinations of direct-acting antiviral agents (DAAs) have been tested for clinical use as novel anti-HCV therapies.[8–10] Emerging data suggest that DAAs, including NS3/4 serine protease inhibitors, NS5B RNA-dependent RNA polymerase inhibitors, and NS5A inhibitors, when used in combination, can achieve significant antiviral activity, but might select for resistance, which can become a primary cause of treatment failure in clinical studies, especially in difficult-to-treat HCV genotypes.[8,9] Additionally, differences in HCV genotypes can result in reduced antiviral activities of certain DAAs and DAA combinations.[11] Therefore, development of additional antiviral agents with diverse resistance profiles and efficacy against a wide spectrum of HCV genotypes is necessary. Major

*Authors share co-first authorship.

Abbreviations used in this paper: cDNA, complementary DNA; DAA, direct-acting antiviral agent; HCV, hepatitis C virus; IC_{50}, 50% inhibitory concentration; PCR, polymerase chain reaction; PEG-IFN, pegylated interferon alfa-2a; RBV, ribavirin; SPT, serine palmitoyltransferase.

0016-5085/$36.00
http://dx.doi.org/10.1053/j.gastro.2013.06.012

efforts are underway to identify novel inhibitors and DAA combinations with a high barrier to resistance for the treatment of HCV infection.

We identified a novel class of serine palmitoyltransferase (SPT) inhibitors derived from fungal metabolites that exhibited HCV replication-inhibiting activity.[12] HCV replication occurs on host cell lipid rafts that form a scaffold for the HCV replication complex. Sphingolipids, the downstream products of SPT action, are essential components of lipid rafts associated with HCV nonstructural proteins on this microdomain. Prevention of the de novo synthesis of sphingolipids by an SPT inhibitor disrupts the HCV replication complex and thereby inhibits HCV replication. This unique mechanism of host enzyme–targeted viral inhibition was hypothesized to have potential for a high barrier to resistance and for antiviral activity across different HCV genotypes. We identified a novel compound, NA808, which is a derivative of the previously described compound NA255 with further improved properties, including improved replicon potency from a 50% effective concentration of 2 nM for NA255 to a 50% effective concentration of 0.84 nM for NA808.[12]

Here, we report the effectiveness of NA808 alone and in combination with DAAs. We used chimeric mice with humanized liver infected with HCV genotype 1a, 1b, 2a, 3a, and 4a to evaluate the potential of NA808 as a novel host-targeted HCV inhibitor.

Materials and Methods

Compounds

NA808 and telaprevir were synthesized by Chugai Pharmaceutical Co., Ltd. (Tokyo, Japan). PEG-IFN was purchased from Chugai Pharmaceutical Co., Ltd. Non-nucleoside polymerase inhibitor, HCV-796, and nucleoside polymerase inhibitor, RO-9187,[13] were synthesized by F. Hoffmann-La Roche Ltd. (Basel, Switzerland).

Development of Drug-Resistance Mutations in HuH7 Cells Harboring Subgenomic Replicon

The HCV subgenomic replicon cell line R6 FLR-N[14] (genotype 1b, HCV-N) was cultured with GlutaMax-I (DMEM-GlutaMax-I; Invitrogen, Carlsbad, CA) containing 10% fetal bovine serum in the presence of 0.5 mg/mL G418 and 48–72 nM NA808 or 1.8–2.7 μM telaprevir at a concentration of 4–6 times the 50% inhibitory concentration (IC_{50}) value for 14 passages. For the replicon assay, cells were seeded in 96-well tissue culture plates, and a 3-fold gradual dilution of NA808 or telaprevir in 5% fetal bovine serum supplemented GlutaMax-I was added. Serial dilutions of both compounds were prepared from the stock solutions dissolved in dimethyl sulfoxide at a concentration of 1 mM for NA808 and 50 mM for telaprevir. Luciferase activity was determined with a Steady-Glo luciferase assay kit (Promega, Madison, WI).

Deep Sequencing of HCV Genomes From Genotype 1b Replicon Cells and Genotype 1a–Infected Chimeric Mice

Deep sequencing of the HCV coding sequences was performed by using the GS Junior System (Roche Diagnostics, Mannheim, Germany), according to manufacturer's instructions. First, the acid guanidinium thiocyanate-phenol-chloroform extraction method was used to extract total RNA from the R6 FLR-N replicon cells after 14 passages with telaprevir or NA808 at a concentration of 6 times the IC_{50} value, or from the liver tissue of HCV-infected chimeric mice that were treated with or without NA808 for 14 days. Complementary DNA (cDNA) was then synthesized from the total RNA with random primers by using Superscript III Reverse Transcriptase (Invitrogen, Life Technologies, Carlsbad, CA). The sequence of nucleotides 3429–9727 of the HCV genotype 1b replicon (R6NRz) genome or nucleotides 325–9381 of the HCV genotype 1a (HCG9) genome, including all of the HCV protein coding sequence, was divided into several segments of 1.5–3 kb with overlapping regions. Four segments of the genotype 1b replicon genome were amplified from the cDNA by polymerase chain reaction (PCR) with specific primers (Supplementary Table 2), and 7 segments of the genotype 1a (HCG9) genome were amplified from the cDNA by nested PCR with the indicated primers (Supplementary Table 3) by using PrimeSTAR GXL DNA Polymerase (TaKaRa Bio, Shiga, Japan). The amplified segments of HCV cDNA were purified from 1% agarose gels by using a MinElute Gel Extraction Kit (Qiagen, Valencia, CA) and quantified by measuring absorbance at 260 nm with a NanoDrop 1000 Spectrophotometer (Thermo Scientific, Wilmington, DE).

The cDNA segments covering the coding sequence of HCV were then pooled together at approximately equimolar ratios. The Covaris S220 system (Covaris, Woburn, MA) was used to shear 500 ng of the pooled cDNA into 700- to 800-bp fragments. The sheared cDNA fragments were purified with the MinElute PCR Purification Kit (Qiagen), ligated with RL MID adaptors (Roche Diagnostics) to prepare the multiple cDNA libraries, and further purified with Agencourt AMPure XP beads (Beckman Coulter, Brea, CA). The quality and quantity of the libraries were assessed by using an Agilent 2100 Bioanalyzer (Agilent Technologies, Santa Clara, CA) and the KAPA Library Quantification Kit (Nippon Genetics, Tokyo, Japan), respectively. The libraries were then subjected to emulsion PCR, and enriched DNA beads (approximately 10% recovery) were loaded onto a picotiter plate and pyrosequenced with a GS Junior sequencer by using titanium chemistry (Roche Diagnostics). Several libraries derived from the HCV genomes generated by different treatments were sequenced in a single GS Junior run. The data obtained were analyzed by the GS Reference Mapper software (Roche Diagnostics) to identify resistant mutations.

SPT Assay

Crude extracts of the HCV subgenomic replicon cell line FLR3-1[12] (genotype 1b, Con-1) were used as a source of SPT in this assay. Briefly, FLR3-1 cells were suspended in HSS buffer (10 mM HEPES-KOH, 25 mM sucrose, and 0.1% sucrose monolaurate) containing 1/100 volume of protease inhibitor cocktail (Sigma, St Louis, MO) and sonicated 10 times with short pulses. After centrifugation at 10,000 rpm for 10 minutes, the supernatant was stored at −80°C until use. Crude extract of FLR3-1 cells was added to 0.015 mL of a reaction mixture containing 200 mM HEPES buffer (pH 8.0), 5 mM EDTA, 10 mM dithiothreitol, 0.05 mM pyridoxal 5-phosphate, 0.05 mM palmitoyl-CoA, and 0.06 mM L-[^{14}C]serine in the presence of NA808. After a 15-minute incubation at 37°C, 0.3 mL chloroform/methanol (1:2, v/v), 0.1 mL phosphate-buffered saline, and 0.1 mL chloroform were added and mixed well. The extracts were

spotted on TLC plates and chromatographed. Radioactive spots were evaluated by using a Bio-imager.

Infection of HCV Genotype 1a, 1b, 2a, 3a, and 4a in Chimeric Mice With Humanized Liver

Chimeric mice were purchased from PhoenixBio Co., Ltd. (Hiroshima, Japan). The mice were generated by transplanting human primary hepatocytes into severe combined immunodeficient mice carrying the urokinase plasminogen activator transgene controlled by an albumin promoter (*Alb-uPA*). HCG9 (genotype 1a, GenBank accession number AB520610), HCR6 (genotype 1b, AY045702), HCR24 (genotype 2a, AY746460), HCV-TYMM (genotype 3a, AB792683), and HCVgenotype4a/KM (genotype 4a, AB795432) were intravenously injected into the chimeric mice with humanized liver at 10^4 (for HCR6, HCR24, HCV-TYMM, and HCVgenotype4a/KM) or 10^6 (for HCR6 and HCG9) copies/mouse. After 4 weeks, the HCV RNA levels in the mice sera had reached approximately 10^8 copies/mL for HCG9 and HCV-TYMM and approximately 10^7 copies/mL for HCR6, HCR24, and HCVgenotype4a/KM. The protocols for animal experiments were approved by our institutional ethics committee. The animals received humane care according to National Institutes of Health guidelines. Patients gave written informed consent before collection of blood or tissue samples.

Administration of NA808 and/or PEG-IFN, Telaprevir, HCV-796, RO-9187 into HCV-Infected Chimeric Mice With Humanized Liver

Treatment was started 12 weeks after HCV inoculation and continued for 14 days. Each treatment group contained at least 3 animals. NA808, PEG-IFN, RO-9187, HCV-796, and telaprevir were administered alone or in combination to chimeric mice infected with HCV genotype 1a (HCG9), genotype 1b (HCR6), genotype 2a (HCR24), genotype 3a (HCV-TYMM), or genotype 4a (HCVgenotype4a/KM). Blood samples and liver samples were collected according to the protocols shown in Supplementary Table 1. All DAAs were used at suboptimal doses to allow the demonstration of synergy when administered in combination therapy.

Quantification of HCV RNA by Real-Time Reverse Transcription PCR

Total RNA was purified from 1 μL chimeric mouse serum by using SepaGene RV-R (Sanko Junyaku Co., Ltd., Tokyo, Japan) and total RNA was prepared from liver tissue by the acid guanidinium thiocyanate-phenol-chloroform extraction method. HCV RNA was quantified by quantitative real-time PCR using techniques reported previously.[15] This technique has a lower limit of detection of approximately 4000 copies/mL for serum. Therefore, all samples in which HCV RNA was undetectable were assigned this minimum value.

Statistical Analysis

Statistical analysis was performed using the Student *t* test. A P value $<.05$ was considered statistically significant.

Results

In Vitro Characteristics of NA808

NA808 (Figure 1*A*), a derivative of NA255 isolated from fungal metabolites of *Fusarium incarnatum* F1476 demonstrated potent antiviral activity in HCV genotype 1b replicon cells with no apparent cellular toxicity under the assay conditions (Supplementary Figure 1*A*) and decreased HCV propagation in genotype 2a HCVcc-producing cells (Supplementary Figure 1*C*). NA255 is a selective inhibitor of SPT that inhibits HCV replication by suppressing the biosynthesis of sphingolipids that are required for HCV replication in replicon cells.[12] NA808 also inhibited the de novo synthesis of sphingolipids (Supplementary Figure 1*B*). According to the resulting Lineweaver-Burk plot of SPT inhibition in a replicon cell lysate, NA808 exhibited a noncompetitive inhibition pattern (Figure 1*B*). These findings suggest that NA808 inhibits HCV replication activities through the prevention of sphingolipid biosynthesis by a noncompetitive inhibition mechanism of SPT.

NA808 Shows a High Barrier to Resistance In Vitro

To evaluate the potential development of resistance to NA808, replicon cells (R6 FLR-N) were cultured in the presence of both G418 and NA808 at a concentration of 4 to 6 times the IC_{50} for 14 passages. Obvious changes in drug sensitivities to NA808 were not observed in these continuously treated replicon cells (Figure 2*A*), and the IC_{50} values were 18.9 nM (no treatment), 14.3 nM (treatment with 4 times the IC_{50}), and 19.8 nM (treatment with 6 times the IC_{50}). In contrast, there was a 5- to 17-fold increase of the IC_{50} values for telaprevir, an NS3/4 serine protease inhibitor, in replicon cells treated with 4 to 6 times the IC_{50} of telaprevir for the same duration (Table 1). The coding sequences of NS3 to NS5B from the replicon system after 14 passages with telaprevir or NA808 were determined by using deep sequencing. The sequences obtained at the 14th passage with telaprevir contained 3 known protease inhibitor resistance mutations (V36A, T54V, and A156T)[16] and NS5 region (Q181H, P223S, and S417P) (Table 2), suggesting that the increase in IC_{50} with telaprevir was accompanied by a shift in viral sequence. In contrast, no significant mutations were found in the 14th passage with NA808. Continuously treated replicon cells developed resistance to telaprevir, but not to NA808.

Anti-HCV Activities of NA808 in Chimeric Mice With Humanized Liver Infected With HCV

To evaluate the anti-HCV effect of NA808 in vivo, we used chimeric mice with humanized liver infected with HCV genotype 1a (HCG9) or 1b (HCR6). The chimeric mice with humanized liver were immunodeficient transgenic uPA/severe combined immunodeficient mice with reconstituted human liver; this mouse model supports long-term HCV infections at clinically relevant titers.

We administered NA808 via intravenous injection according to the schedule shown in Supplementary Table 1. In mice infected with HCV genotype 1a, NA808 (5 mg/kg/d) led to a rapid decrease in serum HCV-RNA (approximately a

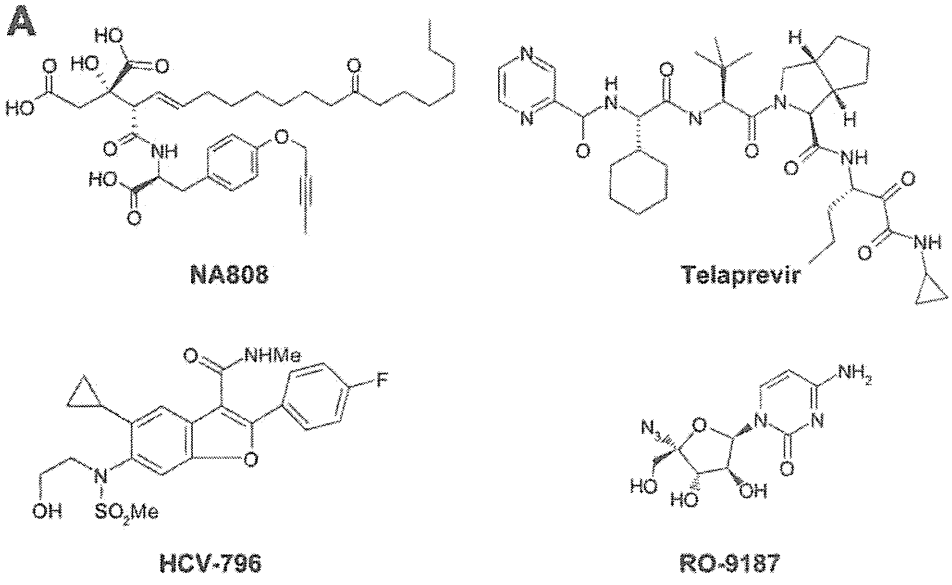

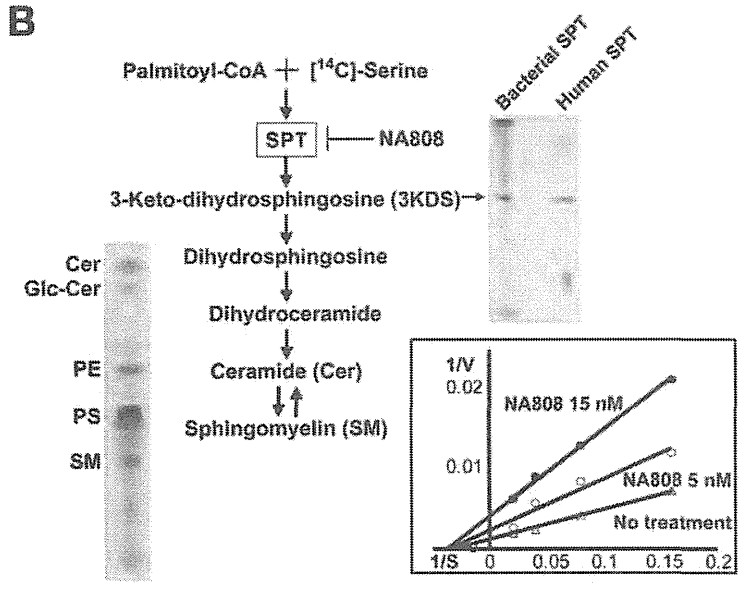

Figure 1. Characteristics of NA808. (*A*) Chemical structures of the compounds used in this study. (*B*) Scheme of de novo sphingolipid biosynthesis and Lineweaver-Burk plot of SPT assay results. Crude extract of FLR3-1 cells was incubated with L-[^{14}C]serine in the presence of NA808. After incubation at 37°C, the extracts were spotted on TLC plates and chromatographed. 3-Keto-dihydrosphingosine (3-KDS) generated from a bacterial SPT reaction is shown as a positive control marker.

2-log decrease within 14 days) (Figure 2*B*). A similar decrease in serum HCV-RNA occurred in mice infected with HCV genotype 1b that were treated with NA808 (5 mg/kg/d) (Figure 2*D*). NA808 also reduced hepatic HCV-RNA at the end of the treatment period in a dose-dependent manner (Figure 2*C* and *E*). These results indicate that NA808 has a robust antiviral effect in chimeric mice with humanized liver infected with HCV genotype 1a or 1b. The most effective dose was 5 mg/kg/d in both genotype 1a– and genotype 1b–infected mice; therefore, we used this dose for further experiments. To address whether NA808 had antiviral activity across HCV genotypes, chimeric mice infected with various strains of HCV were treated with 5 mg/kg of NA808 for 14 days, and then the HCV-RNA levels in the sera were evaluated. Inoculation with several HCV strains, HCG9 (genotype 1a), HCR6 (1b), HCR24 (2a), HCV-TYMM (3a), and HCVgenotype4a/KM (4a), resulted in HCV titers in the sera of mice of approximately 10^8 (HCG9 and HCV-TYMM) and 10^7 (HCR6, HCR24 and HCVgenotype4a/KM) copies/mL, respectively (Supplementary Figure 2, and as described previously[17]). At 14 days after administration, NA808 treatment resulted in approximately 1- to 3-log reductions of serum HCV-RNA in each genotype-infected group (Figure 2*F*). Human serum albumin levels were not changed during the administration period (data not shown), suggesting that the anti-HCV activity of NA808 against several genotypes occurred without any overt toxicity. NA808 was effective and well tolerated in chimeric mice with humanized liver infected with several genotypes of HCV.

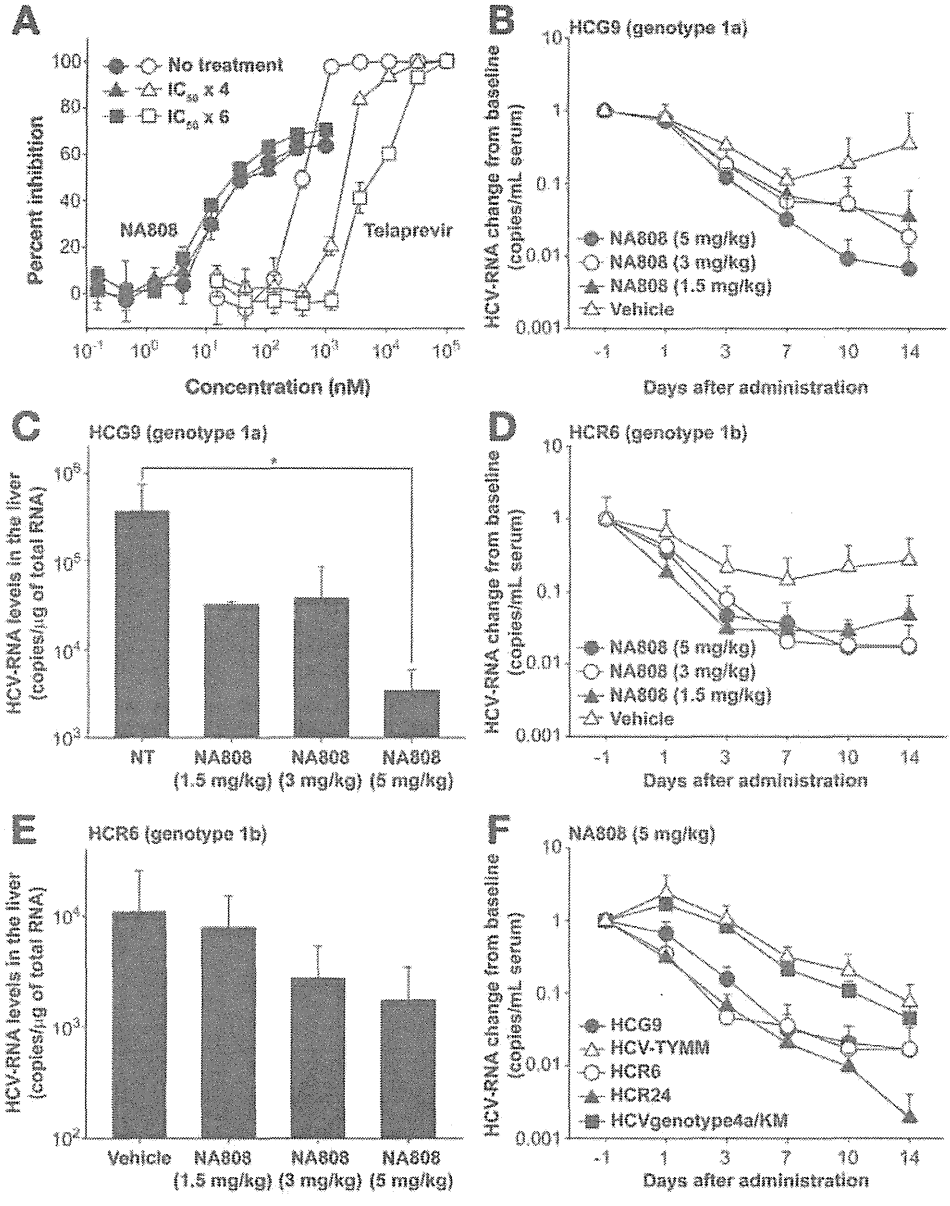

Figure 2. Drug-resistance profile and antiviral effects of NA808 in various HCV genotypes. (*A*) Activities on replicon cells cultured with NA808. Drug-resistant HCV replicons were selected in the presence of G418 and NA808 at a concentration of 4 to 6 times the IC_{50}. Changes in drug sensitivity were examined after the 14th passage. (*B, D*) Time course of serum HCV-RNA levels in chimeric mice infected with HCV genotype 1a (B) or genotype 1b (*D*) treated with vehicle or several doses of NA808 (*closed circles*: 5 mg/kg/d; *open circles*: 3 mg/kg/d; *closed triangles*: 1.5 mg/kg/d; *open triangles*: vehicle). (*C, E*) HCV-RNA levels in the livers of chimeric mice infected with HCV genotype 1a (*C*) or genotype 1b (*E*) at the end of treatment. Error bars = SD (*$P < .05$). (*F*) Time course of serum HCV-RNA levels in the sera of genotype 1a (*closed circles*), 1b (*open circles*), 2a (*closed triangles*), 3a (*open triangle*), and 4a (*closed squares*) after intravenous administration of 5 mg/kg/d NA808. Error bars = SD.

Deep Sequencing of HCV Genotype 1a From Chimeric Mice With Humanized Liver

Full-genome sequence analysis of HCV in the humanized-liver mouse model after 14 days of NA808 administration was performed. The viral RNA was extracted from liver tissues of humanized-liver mice, amplified by using the primer sets shown in Supplementary Table 3 and sequenced with the Roche/454 GS Junior sequencer by using titanium chemistry. We obtained 43,911 and 68,272 sequence reads for HCV genomes from untreated mice and from NA808-treated mice, respectively. The sequences were determined by comparing with the HCG9 reference sequence (GenBank accession number AB520610). As a result, the viral sequences from NA808-treated mice were identical to those from untreated mice.

Table 1. Changes in Drug Sensitivities of HCV Replicon Cells After the 14th Passage in the Presence of NA808 or Telaprevir

Drug	No treatment	IC_{50}×4	IC_{50}×6
NA808 (*nM*)	18.9 ± 2.82	14.3 ± 5.52	19.8 ± 7.86
Telaprevir (*μM*)	0.39 ± 0.022	2.14 ± 0.019	6.48 ± 1.30

Data are indicated as mean ± SD.

Synergistic Effects of NA808 With PEG-IFN or DAAs in Chimeric Mice Infected With HCV

The in vivo synergistic effects of NA808 combined with PEG-IFN on HCV replication were investigated by using chimeric mice with humanized liver infected with HCV genotypes 1a, 2a, and 4a. NA808 was administered

Table 2. Summary of Mutation Frequencies Detected by Using Deep Sequencing for NA808- or Telaprevir-Treated Replicon Cells

Drug	Treatment	Mutation	Region	Frequency (%)
Telaprevir	IC_{50}×6, 14 passages	V36A	NS3	18.1
		T54V	NS3	26.9
		A156T	NS3	12.9
		Q181H	NS5A	25.2
		P223S	NS5A	23.3
		S417P	NS5A	15.8
NA808	IC_{50}×6, 14 passages	Not detected		

Nucleotide sequences based on deep sequencing of NS3 to NS5B region from NA808- or telaprevir-treated replicon cells are compared with untreated controls, and amino acid mutations are shown.

intravenously with or without subcutaneous injection of PEG-IFN for 14 days. In mice infected with HCV genotype 1a, the combination therapy of NA808 with PEG-IFN led to a rapid decrease in serum HCV-RNA of about 4-log within 10 days (Figure 3*A*), and monotherapy with NA808 and PEG-IFN achieved about a 2-log and 1-log decrease, respectively (Figure 4*A*). The levels of serum HCV-RNA were also significantly reduced in genotype 2a- and 4a–infected chimeric mice that received the combination treatment (Figure 3*A*). Although sensitivities to the combination treatment varied according to HCV genotype (1a, 2a, or 4a), the serum HCV-RNA level eventually fell below the level of detection in all mice treated with the combination of NA808 and PEG-IFN (Figure 3*A*); this result was consistent with the significant reductions in hepatic HCV-RNA levels at day 14 (Figure 3*B*).

To determine if NA808 has a synergic effect with DAAs, we examined combination treatment with NS5B nucleoside inhibitor, RO-9187,[13] NS5B polymerase non-nucleoside inhibitor, HCV-796, or NS3/4A protease inhibitor, telaprevir, in HCV genotype 1a- or 1b-infected chimeric mice. Oral administration of once-daily 1000 mg/kg RO-9187, 100 mg/kg HCV-796, or 400 mg/kg telaprevir had only very limited effects or no apparent effects on serum HCV-RNA levels during the 14 days of treatment (Figure 4*B*, *C*, and *D*). However, the combination therapy of NA808 with RO-9187, HCV-796, or telaprevir led to decreases in serum HCV-RNA levels of about 2.6-log, 3.5-log, and 2.5-log, respectively, within 14 days (Figure 4*B*, *C*, and *D*); these reductions were all in excess of viral load reductions achieved by treatment with NA808 (5 mg/kg) alone. After 28 days of combination treatment with NA808 and telaprevir, serum HCV-RNA levels were reduced by 10^4-fold (data not shown). These data suggest that NA808 has synergistic antiviral effects with HCV enzyme-targeted drugs in vivo, regardless of the targeted enzyme. The combination therapy of NA808 with telaprevir and HCV-796 resulted in up to a 4.7-log reduction of serum HCV-RNA within 14 days (Figure 4*D*). At the end of the treatment, hepatic HCV-RNA levels were also reduced, correlating with the reduction of serum HCV-RNA (Figure 4*E*).

Pharmacokinetics Data of Chimeric Mice Treated With NA808

We measured the plasma concentration of NA808 in humanized-liver mice at 24 hours after 14 days of treatment. The plasma concentrations of NA808 at trough level were 0.510 ± 0.517 nmol/L (1.5 mg/kg), 0.446 ± 0.163 nmol/L (3 mg/kg), and 1.44 ± 1.07 nmol/L (5 mg/kg), respectively (Table 3). Obvious toxicological findings in general conditions were not observed at any doses. We selected 1.4 nmol/L as an effective trough level of NA808 in vivo.

Discussion

The current treatment regimen for HCV infection is combination therapy with PEG-IFN and RBV; however, this combination therapy has limited efficacy and is not well tolerated in many patients due to its systemic side-effect profile.[3,4] Although the HCV NS3/4A protease inhibitors telaprevir and SCH503034 (boceprevir) have been recently approved for the treatment of chronic HCV

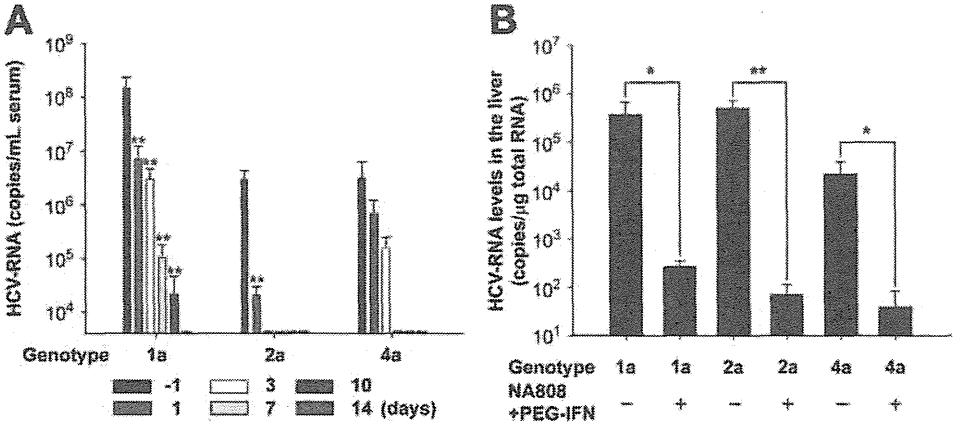

Figure 3. Antiviral effect of combination treatment of NA808 with PEG-IFN on HCV-infected chimeric mice. (*A*) Time course of serum HCV-RNA levels in chimeric mice infected with genotype 1a, 2a, or 4a and treated with a combination of NA808 (5 mg/kg/d, intravenously) and PEG-IFN (30 μg/kg/twice weekly, subcutaneously). HCV-RNA levels one day before administration are shown in *black bars*. (*B*) HCV-RNA levels in the liver 14 days after the initiation of combination therapy with NA808 and PEG-IFN. Error bars = SD. **P* < .05; ***P* < .01.

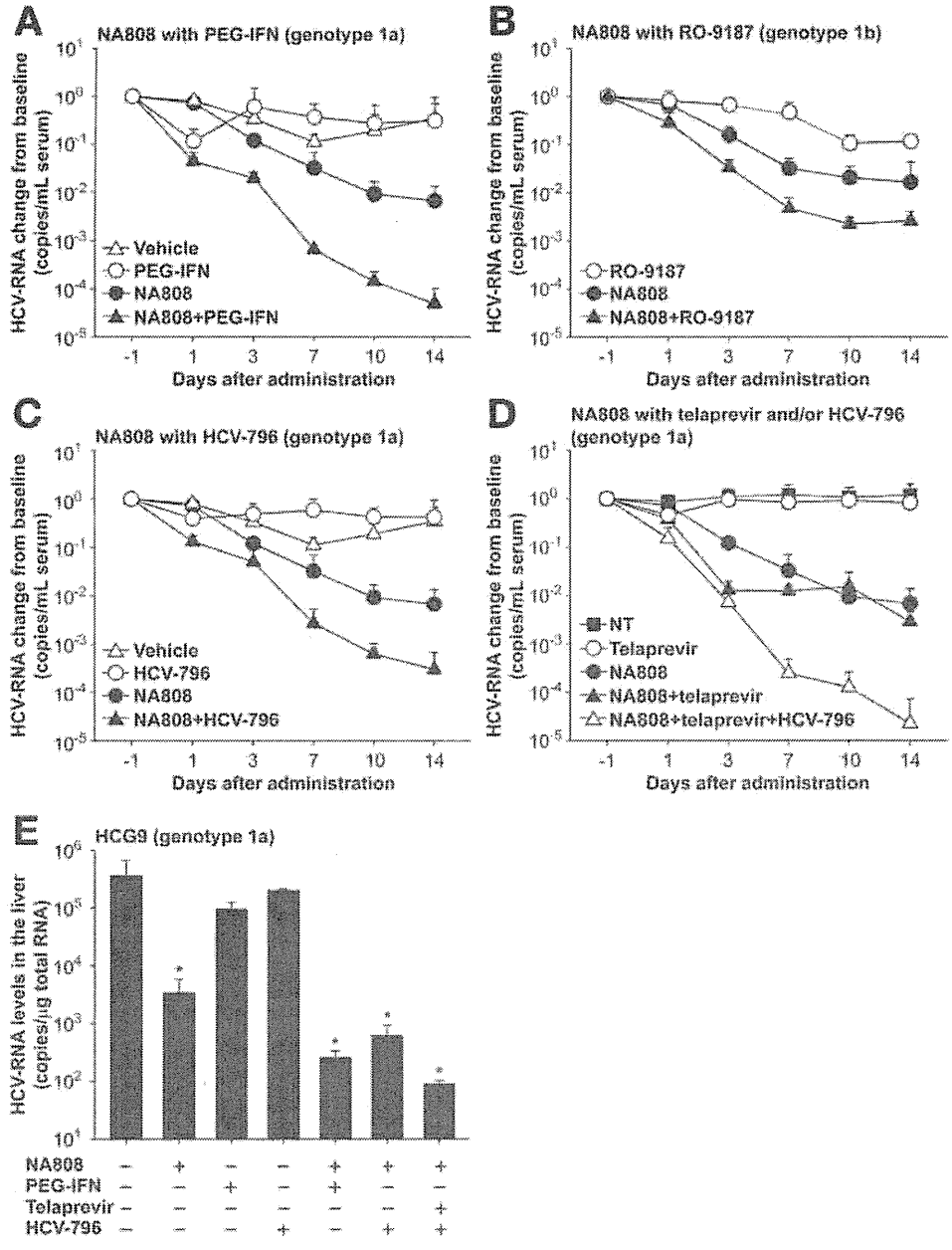

Figure 4. Combination treatment of NA808 with PEG-IFN or direct-acting antiviral agents exhibits robust anti-HCV activity in chimeric mice with humanized liver. (*A–D*) Median change from baseline of serum HCV-RNA over the 14-day monotherapy or combination therapy of NA808 (5 mg/kg/d, intravenously) with PEG-IFN (*A*: 30 μg/kg/twice weekly, subcutaneously), RO-9187 (*B*: 1000 mg/kg/d, orally), HCV-796 (*C*: 100 mg/kg/d, orally), or telaprevir (400 mg/kg/d, orally) and/or HCV-796 (*D*). (*E*) HCV-RNA levels in livers of HCG9-infected chimeric mice at the end of each treatment. Error bars = SD. (*$P < .05$).

infection, these compounds need to be combined with the current standard of care.[5] Therefore, the ultimate goal of developing a therapy for chronic hepatitis C is likely to combine HCV enzyme-targeting agents without the use of IFN or RBV. Currently, combination therapies of DAAs, such as NS3/4 serine protease inhibitors, NS5B RNA-dependent RNA polymerase inhibitors, and NS5A inhibitors, are being tested in clinical trials; however, the emergence of resistance mutations limits the efficacy of these therapies.[8,9] In addition, the antiviral activities of DAAs are reduced for certain HCV genotypes.[11] Additional antiviral agents with high barriers to resistance and potent antiviral activities against a wide variety of HCV genotypes are necessary to establish robust and effective antiviral combination therapies without the use of IFN or RBV. The infection and replication process of HCV can use not only NS3, NS4, and NS5 proteins, but also several known and unknown host protein factors. Drugs that target host protein factors could provide therapies against HCV with a high barrier to resistance.

Table 3. Plasma Concentration of NA808 in Humanized-Liver Mice at 24 Hours After Last Dosing

Dose	Concentration (nmol/L)[a]
1.5 mg/kg	0.510 ± 0.517
3.0 mg/kg	0.446 ± 0.163
5.0 mg/kg	1.44 ± 1.07

[a]Data are indicated as mean ± SD.

In the present study, we evaluated the anti-HCV activity of NA808, a novel host SPT inhibitor in vitro and in vivo. The inhibitory activity of NA808 is attributed to the inhibition of the cellular enzyme SPT, which is necessary for viral replication. The mode of action of NA255, a lead compound of NA808, is the disruption of the scaffold where the HCV replication complex forms on host cellular lipid rafts.[12] NA808 potently inhibits the de novo biosynthesis of cellular sphingolipids, such as ceramide and sphingomyelin, in a dose-dependent manner (Supplementary Figure 1*B*). We have recently reported that NA808 influences sphingolipid metabolism in host cells along with its biosynthesis and that sphingomyelin, a type of sphingolipid, plays a multifaceted role in the HCV life cycle.[18] Additionally, the alteration of sphingolipid metabolism contributes to virion maturation and infectivity in the JFH-1 culture system.[19] These results suggest that NA808 affects many phases of the life cycle, including entry, replication, and maturation. It seems that these diverse working points in the HCV life cycle along with the differentials of the target site could be a reason for the enhanced anti-HCV activity of combination treatment with NA808 and DAAs.

Myriocin, another SPT inhibitor, strongly reduces the expression of hemagglutinin and neuraminidase of influenza virus glycoproteins and inhibits the release of virus particles from infected cells.[20] The mechanism of inhibition involves the sphingomyelin biosynthetic pathway, which plays a critical role in the generation of influenza virus particles. In another report, Miller et al found that ebola virus particles strongly associate with the sphingomyelin-rich regions of the cell membrane and that depletion of sphingomyelin reduces ebola virus infection.[21] Lipid rafts, sphingolipid-enriched membrane microdomains, are involved in the entry, assembly, and budding of various types of viruses other than HCV, including several viruses with a serious public health concern. SPT inhibitors, such as NA808, have the potential to affect the life cycle of the other families of viruses and provide therapeutic options for these difficult-to-treat viral infections via the inhibition of sphingolipid biosynthesis and modification of its metabolism, as described here.

Based on the mechanism of action, NA808 could be anticipated to have antiviral activity against a wide variety of HCV genotypes as compared with DAAs. To estimate the effects of NA808 in DAA combination therapy without the use of IFN or RBV, a combinatorial treatment with NA808 and NS5B polymerase inhibitors and/or NS3/4A protease inhibitors was evaluated in chimeric mice with humanized liver infected with HCV. Both non-nucleoside inhibitors and nucleoside inhibitors of NS5B are currently being tested in clinical trials, and the most advanced protease inhibitors, such as telaprevir, are linear compounds and are currently on the market; several macrocyclic compounds are being tested in clinical trials.[11,22–25] Monotherapy with the non-nucleoside polymerase inhibitor, HCV-796, showed less than a 0.5 $\log_{10}$ reduction of serum HCV RNA levels, while a combined treatment with NA808 reduced the HCV titer by 1000-fold from the initial serum levels. This effect was higher than the effect of NA808 alone and higher than the sum of NA808 and HCV-796 monotherapy effects, suggesting synergistic antiviral efficacy. A similar effect was observed by combination of NA808 with nucleoside polymerase inhibitor, RO-9187, as shown in Figure 4*B*. The maximum reductions in HCV RNA are mediated by triple combinatorial treatment and the significant in vivo anti-HCV activity with combination treatment is also observed when NA808 is combined with PEG-IFN. These observations suggest that NA808 may have synergistic antiviral activity with various classes of anti-HCV agents, regardless of their inhibition mechanism, due to the unique host enzyme-targeted mechanism of action. In addition, NA808 could be expected to show a higher barrier to the development of resistant clones. Deep-sequencing analysis showed no evidence for the development of NA808 resistance after 14 passages in HCV replicon cells, while telaprevir treatment resulted in the selection of known protease resistance mutations (V36A, T54V, and A156T) (Table 2). The full-genome sequence of HCV obtained at day 14 from HCV-infected humanized-liver mice treated with NA808 for 14 days also showed no evidence for the selection of resistance mutations, consistent with the viral load kinetics (Figure 2B).

Host enzyme inhibition might be associated with mechanism-related toxicities or side effects. Although more thorough analyses of toxicity with NA808 are warranted, NA808 did not affect host cell viability in vitro under the assay conditions used (Supplementary Figure 1*A*), and it was well-tolerated in vivo at the efficacious dose used. The effective plasma concentration of NA808 at trough level was approximately 1.4 nmol/L (Table 3), around 100 times lower than rats that received 40 mg/kg NA808 at 24 hours after injection (data not shown). No NA808-related changes, including abnormalities of general conditions, body weight decreases, and macroscopic or microscopic changes were observed at this high dose in rats. Homozygous knockout mice for sptlc1 and sptlc2, subunits of SPT, were embryonic lethal, and heterozygous mice showed no phenotype.[26] Mice with conditional sptlc2 knockout showed necrotic lesions in gastrointestinal cells.[27] The highly selective distribution of NA808 to the liver can contribute to limit potential systemic toxicities associated with SPT inhibition by NA808.[28]

In conclusion, NA808 mediates potent anti-HCV activities in a variety of genotypes with an apparent high barrier to resistance. Synergistic effects with PEG-IFN, HCV protease, and/or polymerase inhibitors are observed in chimeric mice with humanized liver infected with HCV. These findings suggest that NA808 has potential as a novel host-targeted drug in the treatment of HCV infection. NA808 is considered a promising candidate for DAA combination treatment without the use of IFN or RBV to prevent the development of drug resistance and effectively inhibit a wide spectrum of HCV genotypes.

Supplementary Material

Note: To access the supplementary material accompanying this article, visit the online version of *Gastroenterology* at www.gastrojournal.org, and at http://dx.doi.org/10.1053/j.gastro.2013.06.012.

References

1. Wasley A, Alter MJ. Epidemiology of hepatitis C: geographic differences and temporal trends. Semin Liver Dis 2000;20:1-16.
2. Alter MJ, Kruszon-Moran D, Nainan OV, et al. The prevalence of hepatitis C virus infection in the United States, 1988 through 1994. N Engl J Med 1999;341:556-562.
3. Fried MW, Shiffman ML, Reddy KR, et al. Peginterferon alfa-2a plus ribavirin for chronic hepatitis C virus infection. N Engl J Med 2002; 347:975-982.
4. Manns MP, McHutchison JG, Gordon SC, et al. Peginterferon alfa-2b plus ribavirin compared with interferon alfa-2b plus ribavirin for initial treatment of chronic hepatitis C: a randomised trial. Lancet 2001;358:958-965.
5. **Hezode C, Forestier N**, Dusheiko G, et al. Telaprevir and peginterferon with or without ribavirin for chronic HCV infection. N Engl J Med 2009;360:1839-1850.
6. Kwo P, Lawitz J, McCone J, et al. 44th Annual Meeting of the European Association for the Study of the Liver, Copenhagen, Denmark, 22 to 26 April 2009, abstract 4.
7. Sarrazin C, Zeuzem S. Resistance to direct antiviral agents in patients with hepatitis C virus infection. Gastroenterology 2010;138:447-462.
8. Pawlotsky JM. Treatment failure and resistance with direct-acting antiviral drugs against hepatitis C virus. Hepatology 2011;53:1742-1751.
9. Zeuzem S, Buggisch P, Agarwal K, et al. The protease inhibitor GS-9256 and non-nucleoside polymerase inhibitor tegobuvir alone, with RBV or peginterferon plus RBV in hepatitis C. Hepatology 2012; 55:749-758.
10. Gane EJ, Roberts SK, Stedman CA, et al. Oral combination therapy with a nucleoside polymerase inhibitor (RG7128) and danoprevir for chronic hepatitis C genotype 1 infection (INFORM-1): a randomised, double-blind, placebo-controlled, dose-escalation trial. Lancet 2010; 376:1467-1475.
11. Gottwein JM, Scheel TK, Jensen TJ, et al. Differential efficacy of protease inhibitors against HCV genotypes 2a, 3a, 5a, and 6a NS3/4A protease recombinant viruses. Gastroenterology 2011;141: 1067-1079.
12. Sakamoto H, Okamoto K, Aoki M, et al. Host sphingolipid biosynthesis as a target for hepatitis C virus therapy. Nat Chem Biol 2005; 1:333-337.
13. Klumpp K, Kalayanov G, Ma H, et al. 2'-deoxy-4'-azido nucleoside analogs are highly potent inhibitors of hepatitis C virus replication despite the lack of 2'-alpha-hydroxyl groups. J Biol Chem 2008; 283:2167-2175.
14. Watanabe T, Sudoh M, Miyagishi M, et al. Intracellular-diced dsRNA has enhanced efficacy for silencing HCV RNA and overcomes variation in the viral genotype. Gene Ther 2006;13:883-892.
15. Takeuchi T, Katsume A, Tanaka T, et al. Real-time detection system for quantification of hepatitis C virus genome. Gastroenterology 1999;116:636-642.
16. Halfon P, Lacarnini S. Hepatitis C virus resistance to protease inhibitors. J Hepatol 2011;55:192-206.
17. **Inoue K, Umehara T**, Ruegg UT, et al. Evaluation of a cyclophilin inhibitor in hepatitis C virus-infected chimeric mice in vivo. Hepatology 2007;45:921-928.
18. Hirata Y, Ikeda K, Sudoh M, et al. Self-enhancement of hepatitis C virus replication by promotion of specific sphingolipid biosynthesis. PLoS Pathog 2012;8:e100286.
19. Aizaki H, Morikawa K, Fukasawa M, et al. Critical role of virion-associated cholesterol and sphingomyelin in hepatitis C virus infection. J Virol 2008;82:5715-5724.
20. Tafesse FG, Sanyal S, Ashour J, et al. Intact sphingomyelin biosynthetic pathway is essential for intracellular transport of influenza virus glycoproteins. Proc Natl Acad Sci U S A 2013; 110:6406-6411.
21. Miller ME, Adhikary S, Kolokoltsov AA, et al. Ebolavirus requires acid sphingomyelinase activity and plasma membrane sphingomyelin for infection. J Virol 2012;86:7473-7483.
22. Villano SA, Raible D, Harper D, et al. Antiviral activity of the non-nucleoside polymerase inhibitor, HCV-796, in combination with pegylated interferon alfa-2b in treatment-naive patients with chronic HCV. J Hepatol 2007;46:S24.
23. Shi ST, Herlihy KJ, Graham JP, et al. Preclinical characterization of PF-00868554, a potent nonnucleoside inhibitor of the hepatitis C virus RNA-dependent RNA polymerase. Antimicrob Agents Chemother 2009;53:2544-2552.
24. Le Pogam S, Seshaadri A, Ewing A, et al. RG7128 alone or in combination with pegylated interferon-alpha 2a and ribavirin prevents hepatitis C virus (HCV) replication and selection of resistant variants in HCV-infected patients. J Infect Dis 2010;202: 1510-1519.
25. Lam AM, Murakami E, Espiritu C, et al. PSI-7851, a pronucleotide of beta-D-2'-deoxy-2'-fluoro- 2'-C-methyluridine monophosphate: a potent and pan-genotype inhibitor of hepatitis C virus replication. Antimicrob Agents Chemother 2010;54:3187-3196.
26. Hojjati MR, Li Z, Jiang XC, et al. Serine palmitoyl-CoA transferase (SPT) deficiency and sphingolipid levels in mice. Biochim Biophys Acta 2005;1737:44-51.
27. Ohta E, Ohira T, Matsue K, et al. Analysis of development of lesions in mice with serine palmitoyltransferase (SPT) deficiency -Sptlc2 conditional knockout mice-. Exp Anim 2009;58:515-524.
28. Ozeki K, Okano K, Ohminato N, et al. The mechanism of the liver specific distribution of NA808, a first-in-class serine palmitoyltransferase inhibitor, mediated by organic anion transporter 1B1-multidrug resistance associated protein 2. Hepatology 2011; 54:550A.

Author names in bold designate shared co-first authorship.

Received June 16, 2012. Accepted June 10, 2013.

Reprint requests

Address requests for reprints to: Michinori Kohara, PhD, Department of Microbiology and Cell Biology, Tokyo Metropolitan Institute of Medical Science, 2-1-6 Kamikitazawa, Setagaya-ku, Tokyo 156-8506, Japan. e-mail: kohara-mc@igakuken.or.jp; fax: +81 3 5316 3137.

Acknowledgments

The authors would like to thank Yoshimi Tobita and Hiroshi Yokomichi for their technical assistance.

Conflicts of interest

The authors disclose the following: A. Katsume, K. Okamoto, Y. Ohmori, S. Fujiwara, T. Tsukuda, Y. Aoki, and M. Sudoh are employees of Chugai Pharmaceutical Co., Ltd. I. Kusanagi is an employee of Chugai Research Institute for Medical Science Inc. K. Klumpp is an employee of F. Hoffmann-La Roche Inc. The remaining authors disclose no conflicts.

Funding

This study was supported in part by a grant from the Ministry of Education, Culture, Sports, Science (213901457) and Technology of Japan and a grant from the Ministry of Health, Labour and Welfare of Japan.

Genes to Cells

4E-BP1 regulates the differentiation of white adipose tissue

Kyoko Tsukiyama-Kohara[1,2]*, Asao Katsume[3], Kazuhiro Kimura[4], Masayuki Saito[5] and Michinori Kohara[6]

[1]*Department of Experimental Phylaxiology, Faculty of Medical and Pharmaceutical Sciences, Kumamoto University, 1-1-1 Honjo, Kumamoto-City, Kumamoto 860-8556, Japan*
[2]*Transboundary Animal Diseases Centre, Joint Faculty of Veterinary Medicine, Kagoshima University, 1-21-24 Korimoto, Kagoshima 890-0065, Japan*
[3]*Fuji Gotemba Research Labs, Chugai Pharmaceutical Co. Ltd, 135, Komakado, 1 chome, Gotemba-shi, Shizuoka 412-8513, Japan*
[4]*Department of Biomedical Sciences, Graduate School of Veterinary Medicine, Hokkaido University, 18-9 Kita-Ku, Sapporo, Hokkaido 060-0818, Japan*
[5]*Department of Nutrition, School of Nursing and Nutrition, Tenshi College, Sapporo 065-0013, Japan*
[6]*Department of Microbiology and Cell Biology, Tokyo Metropolitan Institute of Medical Science, 2-1-6 Kamikitazawa, Setagaya-ku, Tokyo 156-8506, Japan*

4E Binding protein 1 (4E-BP1) suppresses translation initiation. The absence of 4E-BP1 drastically reduces the amount of adipose tissue in mice. To address the role of 4E-BP1 in adipocyte differentiation, we characterized 4E-BP1$^{-/-}$ mice in this study. The lack of 4E-BP1 decreased the amount of white adipose tissue and increased the amount of brown adipose tissue. In 4E-BP1$^{-/-}$ MEF cells, PPARγ coactivator 1 alpha (PGC-1α) expression increased and exogenous 4E-BP1 expression suppressed PGC-1α expression. The level of 4E-BP1 expression was higher in white adipocytes than in brown adipocytes and showed significantly greater up-regulation in white adipocytes than in brown adipocytes during preadipocyte differentiation into mature adipocytes. The amount of PGC-1α was consistently higher in HB cells (a brown preadipocyte cell line) than in HW cells (a white preadipocyte cell line) during differentiation. Moreover, the ectopic over-expression of 4E-BP1 suppressed PGC-1α expression in white adipocytes, but not in brown adipocytes. Thus, the results of our study indicate that 4E-BP1 may suppress brown adipocyte differentiation and PGC-1α expression in white adipose tissues.

Introduction

The translation of eukaryotic messenger RNA (mRNA) requires a 7-methyl guanosine residue cap structure at the 5′ end of the mRNA to which eukaryotic initiation factors (eIFs) can bind. In particular, the ribosomal subunits associated with eIF4G and cap-bound eukaryotic initiation factor 4E (eIF4E) are required for cap-dependent translation. The eIF4E inhibitory proteins (Pause *et al.* 1994; Poulin *et al.* 1998) and the eIF4E-binding proteins [4E binding proteins (4E-BPs)] prevent eIF complex formation by sequestering the available eIF4E (Haghighat *et al.* 1995; Mader *et al.* 1995).

Communicated by: Yo-ichi Nabeshima
**Correspondence*: kkohara@agri.kagoshima-u.ac.jp

Signaling from growth factors, hormones, mitogens and cytokines can cause hyperphosphorylation of 4E-BPs through the activation of either phosphoinositide 3′-OH kinase (PI3K) (Mader *et al.* 1995; von Manteuffel *et al.* 1997; Gingras *et al.* 1998) or the serine/threonine kinase Akt/protein kinase B (PKB) (Gingras *et al.* 1998; Kohn *et al.* 1998; Dufner *et al.* 1999; Takata *et al.* 1999). The phosphorylation of 4E-BP1 is also dependent on the FKBP12-rapamycin–associated protein/mammalian target of rapamycin (FRAP/mTOR) kinase (Mendez *et al.* 1996; Brunn *et al.* 1997a,b; Hara *et al.* 1997; Burnett *et al.* 1998; Gingras *et al.* 1998), which can be activated by hormones such as insulin and amino acids such as leucine (Proud 2004). Hyperphosphorylated 4E-BP1 subsequently abrogates interaction with eIF4E and increases the rate of cap-dependent translation (Lin

DOI: 10.1111/gtc.12059

et al. 1994; Pause *et al.* 1994; Fadden *et al.* 1997). 4E-BP1 is involved in endoplasmic reticulum (ER) stress-induced apoptosis in pancreatic β cells through transcription factor ARF4 (Yamaguchi *et al.* 2008).

We previously described a major role of 4E-BP1 *in vivo*, whereby an increase in the metabolic rate and decrease in the amount of white adipose tissue (WAT) were observed in male 4E-BP1$^{-/-}$ mice (Tsukiyama-Kohara *et al.* 2001). Here, we have characterized the role of 4E-BP1 in the regulation of adipocyte differentiation and showed that its differential effects in white and brown adipocytes occur through the regulation of PGC-1α expression.

Results

Effects of 4E-BP1 on adipose tissues

The disruption of 4E-BP1 decreased the body weight of 10- to 12-month-old mice (Fig. 1A,B), whereby male 4E-BP1$^{-/-}$ mice were particularly affected and had less WAT than wild-type ($^{+/+}$) mice (Fig. 1C).

The histological characterization indicated previously that the amount of multilocular adipocytes that were characteristic of brown adipose tissue (BAT) was significantly increased in the inguinal WAT of 4E-BP1$^{-/-}$ mice (Tsukiyama-Kohara *et al.* 2001).

Effects of 4E-BP1 on PGC-1α expression

Expression of PGC-1α was previously shown to be increased in BAT (Gomez-Ambrosi *et al.* 2001); therefore, in the present study, PGC-1α expression was examined in WT (+/+) and knockout ($^{-/-}$) mouse embryonic fibroblasts (MEF, Fig. 2A,B), as well as in cells transfected with a 4E-BP1 expression vector. The lack of 4E-BP1 significantly increased PGC-1α levels, and exogenous over-expression of 4E-BP1 significantly decreased PGC-1α levels in knockout cells.

Effects of 4E-BP1 on adipocyte differentiation

We further examined the role of 4E-BP1 in adipocyte differentiation. A white preadipocyte cell line (HW cells) and a brown preadipocyte cell line (HB cells) (Irie *et al.* 1999) were differentiated into mature adipocytes (Fig. 3A), and the induction profiles of PGC-1α and 4E-BP1 were characterized during this differentiation (Fig. 3B). The levels of 4E-BP1 and PGC-1α increased from day 0 to day 2; 4E-BP1 expression was consistently higher in HW cells than in HB cells, and PGC-1α expression was higher in HB cells than in HW cells during the 4 days of differentiation. Treatment with norepinephrine (NE) can induce the expression of uncoupling protein (UCP) 1 (Irie *et al.* 1999), which is a BAT-specific protein. We treated HW and HB cells with NE, but it did not significantly influence the expression of 4E-BP1 or PGC-1α.

To examine the effect of 4E-BP1 over-expression, transgene expression in HW and HB cells was characterized (Fig. 4). In particular, the expression of PGC-1α and 4E-BP1 was characterized in these cells (Fig. 4A). Over-expression of 4E-BP1 significantly suppressed the expression of PGC-1α in HW cells, but not in HB cells (Fig. 4B). Ectopic over-expression of 4E-BP1 suppressed the differentiation of HW preadipocytes (Fig. 4C) but did not significantly influence the differentiation of HB preadipocytes (data not shown). Thus, 4E-BP1 may decrease the

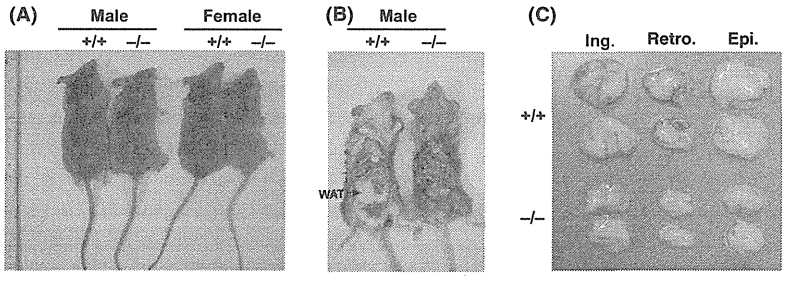

Figure 1 Decrease in adipose tissue in 4E-BP1$^{-/-}$ mice. (A) Male and female wild-type ($^{+/+}$) and 4E-BP1$^{-/-}$ ($^{-/-}$) mice (age, 10–12 months). (B) Intraperitoneal view of wild-type ($^{+/+}$) and 4E-BP1$^{-/-}$($^{-/-}$) male mice. White adipose tissue (WAT) is indicated by an arrow. (C) Inguinal (Ing.), retroperitoneal (Retro.) and epididymal (Epi.) fat pads of wild-type (+/+) and 4E-BP1$^{-/-}$ ($^{-/-}$) male mice.

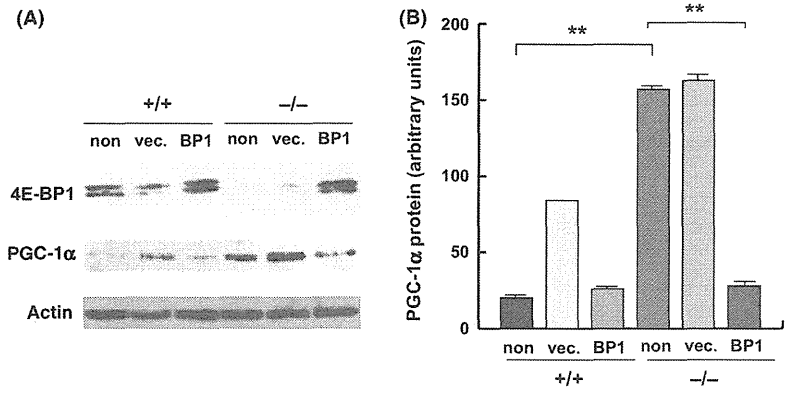

Figure 2 Expression of PGC-1α in wild-type ($^{+/+}$) and 4E-BP1$^{-/-}$ ($^{-/-}$) MEF cells. (A) The 4E-BP1 expression vector and control vector were transfected in cells, and expression was measured 2 days after transfection. (B) Quantification of PGC1α protein expression in ($^{+/+}$) or ($^{-/-}$) MEF cells transfected with the control vector or 4E-BP1 expression vector. The average and S.D. values of 3 samples are indicated. $^{**}P < 0.01$ (two-tailed Student's *t*-test).

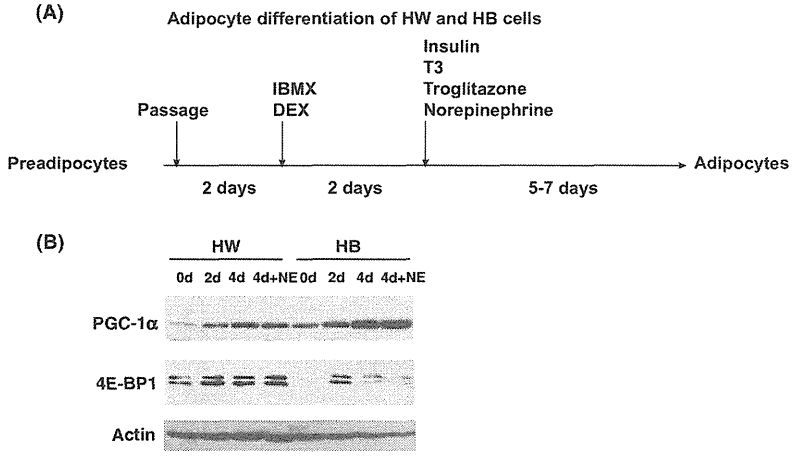

Figure 3 (A) Differential role of 4E-BP1 in adipocyte differentiation and the modulation of PGC-1α expression. Timeline of preadipocyte (HB and HW cells) differentiation into mature adipocytes. (B) Expression of PGC-1α and 4E-BP1 in HW and HB cells after differentiation for 0, 2 and 4 days. NE, norepinephrine (1 μM).

expression of PGC-1α and suppress adipocyte differentiation in WAT but not in BAT (Fig. 4D).

Discussion

As reported in our previous study (Tsukiyama-Kohara *et al.* 2001), the amount of WAT is significantly decreased in male 4E-BP1$^{-/-}$ mice. In the present study, we have further showed that disruption of 4E-BP1 induces the over-expression of PGC-1α. Because previous studies have indicated that PGC-1α over-expression in white adipose cells induces mitochondrial biogenesis and UCP-1 expression (Puigserver *et al.* 1998; Wu *et al.* 1999; Tiraby *et al.* 2003), greater amounts of BAT might be present in these male mice (Tsukiyama-Kohara *et al.* 2001). Moreover, we found that over-expression of 4E-BP1 decreased the expression of PGC-1α in a WAT cell line but not in a BAT cell line. Our results also showed that 4E-BP1 was more abundantly expressed in the WAT cell line during differentiation, whereas PGC-1α was more abundantly expressed in the BAT cell line. Ectopic over-expression of 4E-BP1 suppressed PGC-1α expression in white adipocytes

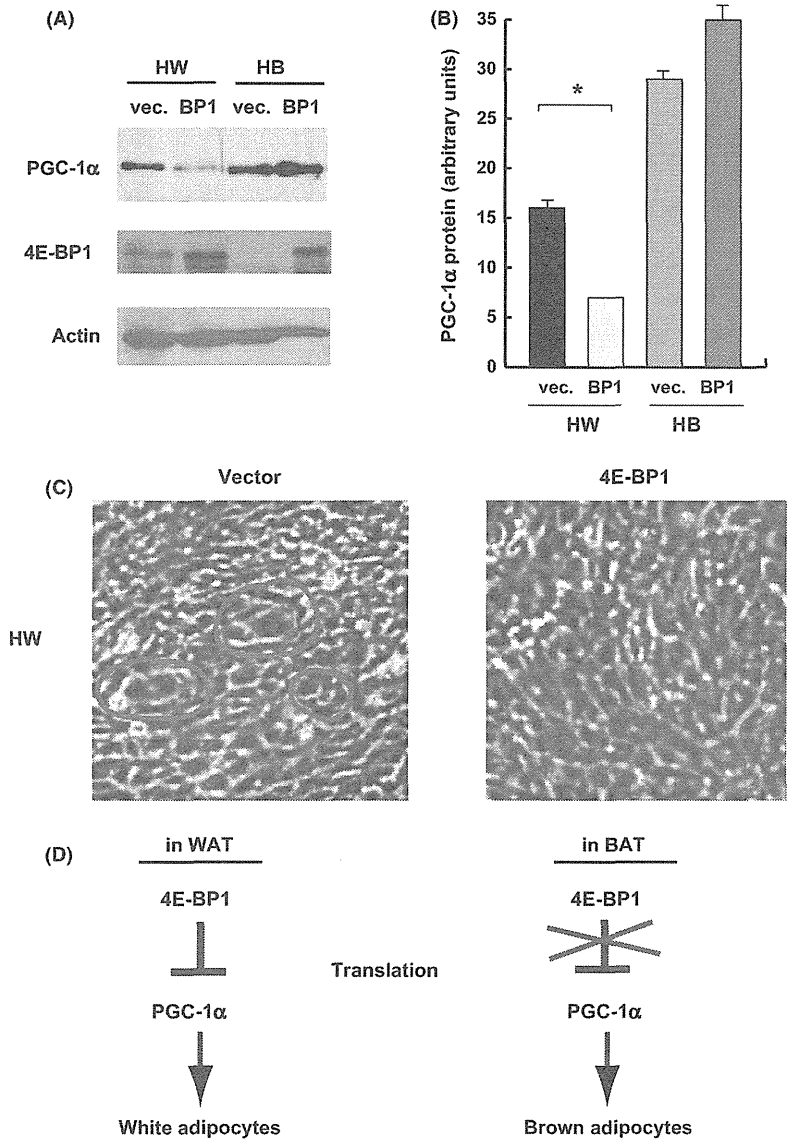

Figure 4 Role of 4E-BP1 in PGC-1α expression and adipocyte differentiation. (A) Expression of PGC-1α in HW and HB cells that were transfected with the control vector or with the 4E-BP1 expression plasmid. Expression levels were measured 2 days after transfection. (B) Quantification of PGC1α protein expression in HW or HB cells transfected with the control vector or 4E-BP1 expression vector. The average and S.D. values for 3 samples are indicated. $^{**}P < 0.05$ (two-tailed Student's *t*-test). (C) Morphological features of differentiated HW cells transfected with the control vector or the 4E-BP1 expression vector at 2 days after differentiation (×40). Red circles indicate differentiating adipocytes, as reported previously (Irie *et al.* 1999). (D) Role of 4E-BP1 in adipocyte differentiation. 4E-BP1 may suppress the expression of PGC-1α and differentiation in white adipose tissue. However, 4E-BP1 does not influence the expression of PGC-1α and differentiation in brown adipose tissue.

but not in brown adipocytes. This differential regulation of PGC-1α expression by 4E-BP1 in white and brown adipocytes might be due to differences in the expression profiles of the host factor in HW and HB cells. Using microarray analysis in a complementary study, we observed such differences in at least 20 factors (Table S1 in Supporting Information).

PGC-1α is highly expressed in brown adipocytes and plays a significant role in adaptive thermogenesis.